MSc Thesis Biobased Chemistry and Technology

Mathematical model of the artificial pancreas; a Utopia?
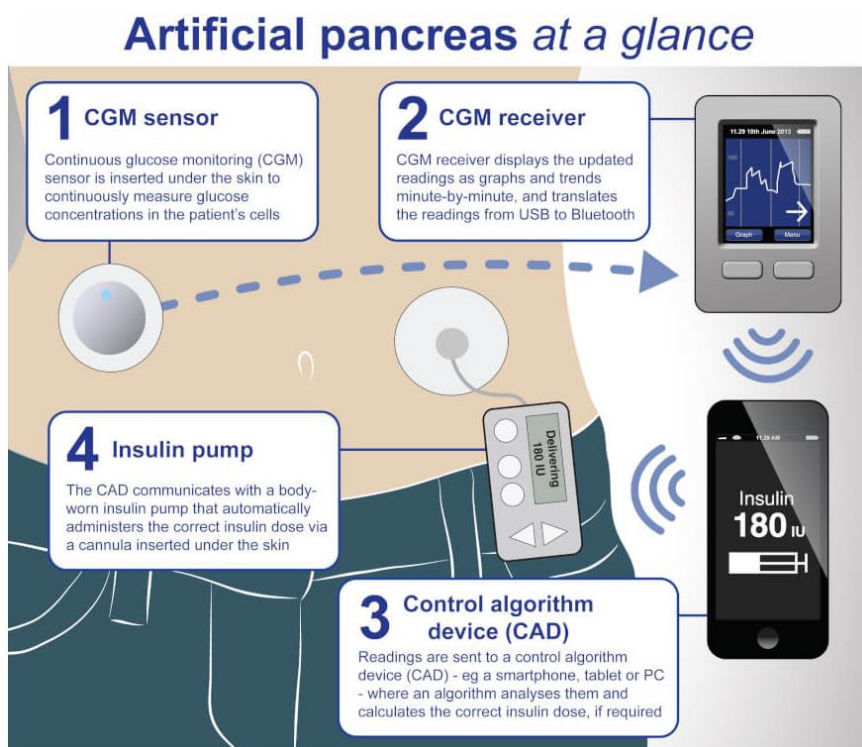
Guido Hendricks

August, 2018

Artificial pancreas *at a glance*

1 CGM sensor
Continuous glucose monitoring (CGM) sensor is inserted under the skin to continuously measure glucose concentrations in the patient's cells

2 CGM receiver
CGM receiver displays the updated readings as graphs and trends minute-by-minute, and translates the readings from USB to Bluetooth

4 Insulin pump
The CAD communicates with a body-worn insulin pump that automatically administers the correct insulin dose via a cannula inserted under the skin

3 Control algorithm device (CAD)
Readings are sent to a control algorithm device (CAD) - eg a smartphone, tablet or PC - where an algorithm analyses them and calculates the correct insulin dose, if required

WAGENINGEN
UNIVERSITY & RESEARCH

Mathematical model of the artificial pancreas; a Utopia?

Name course	:	MSc Thesis Biobased Chemistry and Technology
Number	:	BCT-80439
Study load	:	39 ects
Date	:	July 2018
Student	:	ing. Guido Bart Leonard Hendricks
Registration number	:	800215-323-050
Study programme	:	MAB
Report number	:	071BCT
Supervisors	:	dr. ir. Gerard van Willigenburg
		dr. Rachel van Ooteghem MSc.
Examiner	:	prof. dr. ir. Karel Keesman
Group	:	Biobased Chemistry and Technology
Address	:	Bornse Weilanden 9
		6708 WG Wageningen
		The Netherlands

WAGENINGEN
UNIVERSITY & RESEARCH

Abstract

Euglycemia is controlled by the human body by the hormones insulin and glucagon. The blood glucose (BG) concentration of a Type 1 Diabetes Mellitus (T1DM) will be out of range due to the lack of the hormone insulin. This results in a BG fluctuation. The aim in controlling T1DM is to be in the euglycemic range. A sub-optimal method to control T1DM is to do measurements and administer insulin by hand. Finger pricks are used to determine the BG level. After calculating the carbohydrates and the number of units of insulin, the insulin is administered subcutaneously.

To enhance patients' health-related quality of life (HRQoL) an automated artificial pancreas (AP) should be realized. In this way, the BG level is monitored and controlled around the clock with less patient effort resulting in a better HRQoL. A basic AP setup will consist of a subcutaneous continuous glucose monitor (CGM), a subcutaneous insulin infusion pump and a control algorithm. The goal of this research is to find and calibrate a T1DM patient model using collected patient data, after an extensive literature survey of the glucose-insulin models. This calibrated model is the first step to designing a control strategy.

Patient data were collected from the Rijnstate Hospital in Arnhem and from the literature survey, the Dalla Man, Rizza, et al. Meal Glucose-Insulin Model was examined, adjusted and extended. A T1DM simulation model is developed. After a parameter sensitivity analysis, the sensitive model parameters where selected. A fast program was used to find identifiable parameter sets. Using a patient CGM data and the glucose model outcome, parameter estimation was performed based on, the minimization of the sum of squared errors (SSE). The best fit is chosen, after calculating the absolute value of the minimization of the SSE.

The conclusion is that the best fit of the model will follow the glucose trend of the reference (CGM data) although lower model glucose values are observable. Nevertheless a state of the art calibrating tool set is presented and a solid basis is formed for further AP model enhancement. Also the presented model is very useful for teaching causalities for diabetics and other educational purposes.

Keywords: Diabetes, T1DM modelling, Dalla Man, Glucose Regulatory System

Table of content

1 Introduction

When a meal is consumed a healthy person, the digestive system will break down the carbohydrates into glucose, a simple sugar. The pancreas β cells will release the hormone insulin. Insulin allows the cells of the human body to convert glucose to energy, if needed. If the blood glucose level falls below the basal blood glucose level, glucagon is secreted by the pancreas α cells. The liver is activated by the glucagon hormone and will release the stored glucose, resulting in a steady supply of glucose in the blood plasma (Havard T.H. Chan, 2017). Around the clock, the pancreas will also release a small amount of insulin. This so-called basal insulin secretion will keep the basal blood glucose level steady without a meal intake (Harsh, 2013).

The destruction of the cells β of the pancreas will stop the production of the hormone insulin resulting in Type 1 Diabetes Mellitus (T1DM). T1DM will reduce the patients' Health-Related Quality of Life (HRQoL).

T1DM is a chronic disease and likely starts in childhood (5-7 years of age or near puberty). Because of this peak in presence, it is also known as juvenile Diabetes Mellitus (DM). The Epidemiology of the disease is not equally divided over the world population. Environmental influences affect the incidence rate, the underlying mechanisms are however unknown. For example, T1DM scores the highest in Finland, over 60 cases per 100.000 people each year, versus the lowest rating in China, 0 to 1 cases per 100.000 people each year, visualized in Figure 1 and Figure 2 (Atkinson, Eisenbarth, & Michels, 2014; Väisänen, 2015).

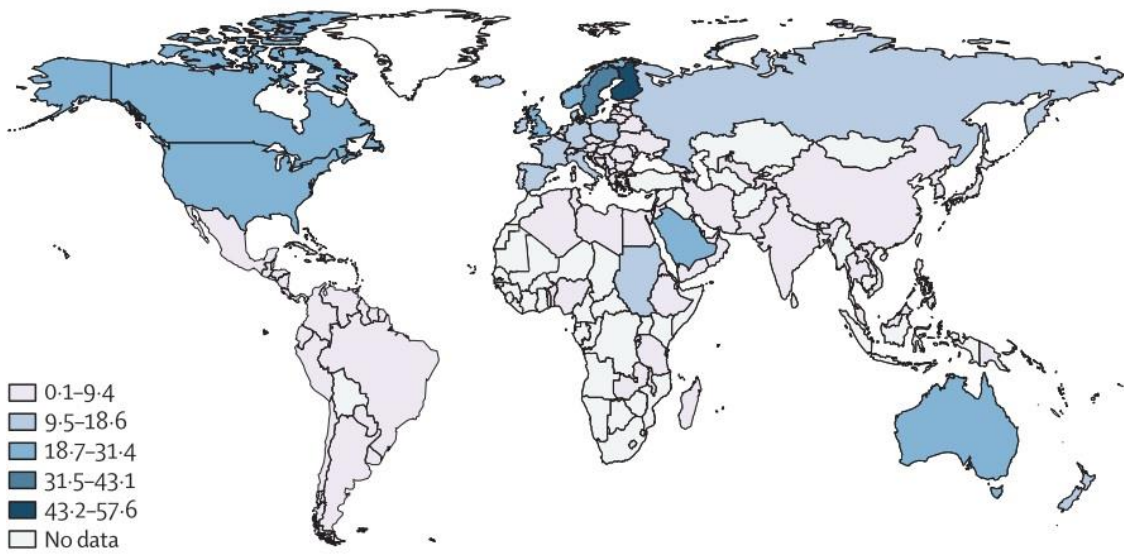**Figure 1.** **The incidence of T1DM in children aged 0−14 years, by region.**

The estimated global incidence of type 1 diabetes, by region, in 2011 (Atkinson et al., 2014).

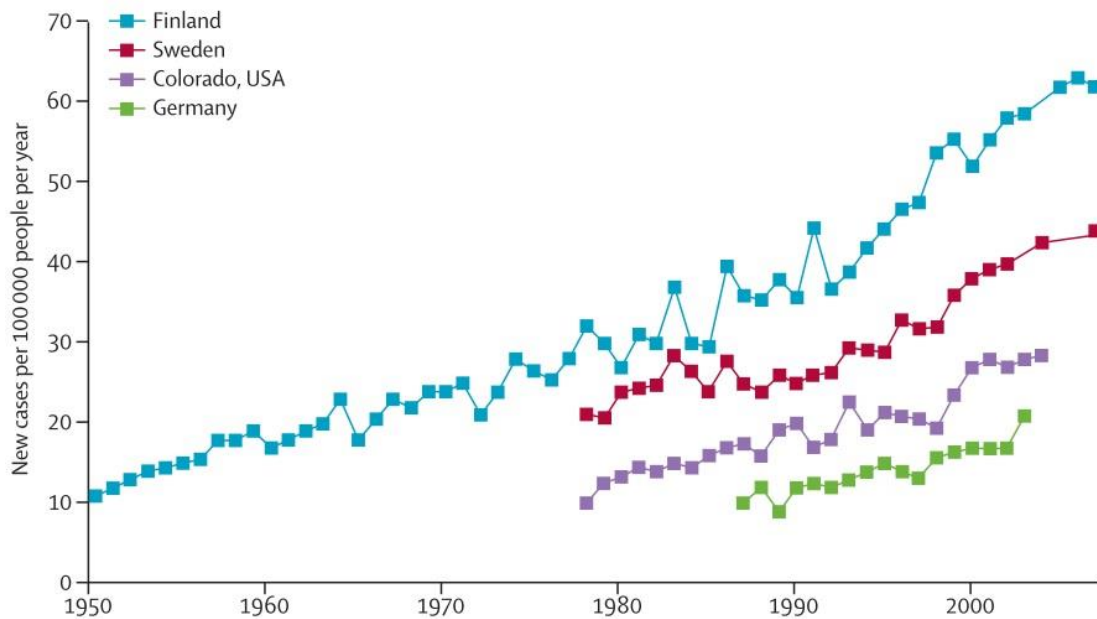

Figure 2. **The incidence of T1DM in children aged 0−14 years, over time.**

Time-based trends for the incidence of type 1 diabetes in children ages 0-14 years in areas with high or high-intermediate rates of disease (Atkinson et al., 2014).

1.1 The Pancreas

The pancreas consists of different tissues. The major two tissues are the acini (exocrine gland) and the islets of Langerhans (endocrine gland). The acini produce the digestive enzymes and the islets of Langerhans produce the hormones insulin, glucagon and somatostatin.

1.1.1 Islets of Langerhans

The German anatomist Paul Langerhans (1847-1888) found islets in the pancreas in the year 1869. After his discovery, these islets were named after the founder and referred to as the islets of Langerhans. The islets are small groups of cells that produce hormones. The alpha cells secrete glucagon, the beta cells secrete insulin and amylin and the delta cells secrete somatostatin. Pancreatic Polypeptide (PP) is also secreted from the islets of Langerhans. The human pancreas has 1 to 2 million islets of Langerhans, which are placed around small capillaries through which its cells secrete their hormones (David Darling, 2016; Guyton & Hall, 2006).
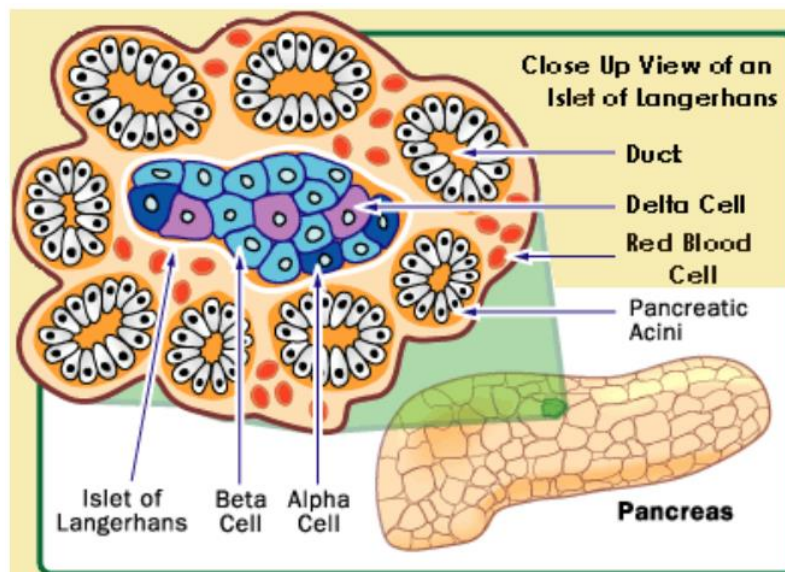
Figure 3.   Islet of Langerhans (David Darling, 2016).

The pancreatic β cells of the islets of Langerhans will produce the hormone insulin as mentioned before. There is a direct cell-to-cell communication between the different cells in the islets of Langerhans. Therefore, the production of the different hormones will react to the production of the others. The insulin production will inhibit the production of glucagon while amylin inhibits the insulin

production. Somatostatin will inhibit both insulin and glucagon (Guyton & Hall, 2006).

When glucagon is secreted into the bloodstream, the liver will metabolize the glycogen to glucose. After insulin is secreted into the bloodstream, the liver and muscular tissue will convert and absorb glucose into glycogen. The rest (excess) of the glucose will be converted to fat by the stimuli of the hormone insulin (Guyton & Hall, 2006). For regulating the fluctuation of the glucose level in the blood, a fast and short reacting hormone like insulin is necessary. When insulin is secreted into the bloodstream, it has a half-time of about 6 minutes. This is important because the blood glucose level is changing fast over a short time. The destruction of the pancreatic β cells will result in insulin insufficiency. The lack of insulin secretion develops type 1 diabetes mellitus (T1DM), a chronic disease (Atkinson et al., 2014). A lifetime of insulin administering treatment is necessary and will reduce the HRQoL of the patient.

1.1.2 The Pancreas and Diabetes Mellitus

The pancreas, see Figure 4, has two main functions: regulating the blood glucose level and releasing enzymes for digesting purposes of the human body. Hereby the pancreas is an exocrine as well as an endocrine gland. For regulating the blood glucose level or body metabolism, the pancreas produces the hormones insulin, glucagon and others (Guyton & Hall, 2006).
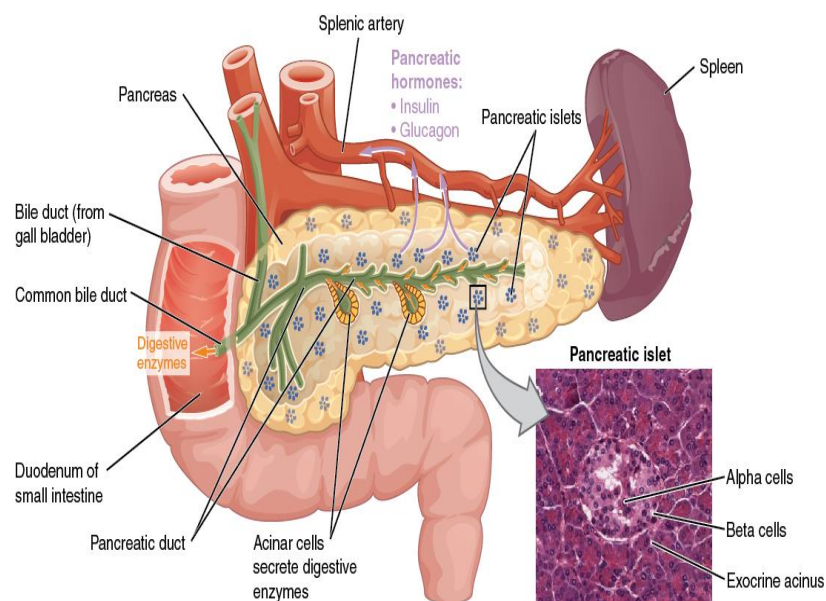

Figure 4.   The pancreas (Pharma Tips 2013).

When an abnormality in the production of insulin occurs, the BG (blood glucose) level of the human body is not controllable anymore. The blood glucose level will increase when an insufficient amount of insulin is present to convert glucose to energy by the tissue cells of the human body. This high level of BG and the absence of the hormone insulin is called Type 1 Diabetes Mellitus (T1DM), also known as insulin dependent diabetes mellitus.

In general, there are two types of DM: type 1 and type 2. T1DM is caused by the destruction of the pancreatic beta cells (β cells) resulting in no more secretion of the hormone insulin by the defective β cells of the pancreas. Type 2 diabetes mellitus (T2DM) is an increase of insulin resistance of the cells of the human body. To reduce the blood glucose level of T2DM, body weight control and administering of insulin are essential.

In the early times, the medical diagnose of DM was by smelling and tasting the urine. The urine of the patient will be sweet when tasted, since due to the kidney membrane failure, glucose is passing the kidney glomerular basement membrane (GBM). If the blood glucose level is too high for a long time, it will damage the GBM and other organs in the human body.

Aretaeus describes the disease Diabetes clearly in 150 AD and referred if to 'melting down of the flesh and limb into urine'. Doctor Tomas Willes (1621-1675) correlated the sweetness of urine to the illness of Diabetes and renamed the disease Diabetes to Diabetes Mellitus. In Greek Mellitus means 'like honey', and diabetes 'syphoned out' (Canadian Diabetes Association, 2017; Gale, 2014; Roberts, 2015).

Symptoms associated with DM are polydipsia (excessive fluid intake), polyphagia (excessive hunger) and polyuria (an increase in the production of urine and the passage of it). If DM is diagnosed, the blood glucose level is higher than 7 mmol/L (Atkinson et al., 2014); the human body is not able to control the correct blood glucose level of 4-6 mmol/L, also known as normoglycemia.

1.2 Insulin dose calculations by hand

Carbohydrates (CHO) are found in cereals, fruit, dairy, bread, cake, soft drinks and pastry for example. One gram of CHO yields 16 kJ or 3.75 kcal. To reduce

the blood glucose level of T1DM, insulin is administered according to the carbohydrate intake by the patient. Patient wise insulin recommendations and calculations need to be fine-tuned depending on the patient's resistance to insulin. The patient needs to understand its disease and other factors that have a positive or negative effect on the treatment of its T1DM. The patient is in the lead to maintain its glucose balance at a normal level around the clock. It is like standing on a balancing board; stabilizing it means dealing with many internal and external factors. This balancing board is depicted in Figure 5.

Commonly used formulas to create insulin dose recommendations for patients will be: the total daily insulin dose, the basal insulin dose, the rule of 500 and the rule of 1800 (Kennedy, Bedrich, Gray, Kroon, & Demetsky, 2017). In this chapter, these formulas are explained and used as a rule of thumb for patients.
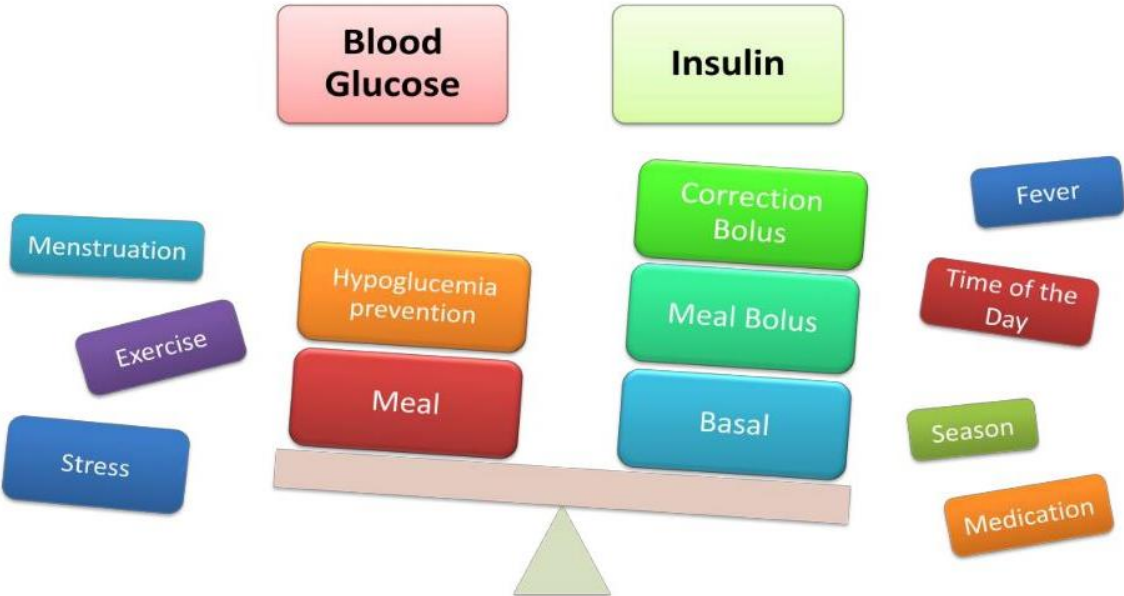
Figure 5.   The balancing equation (Väisänen, 2015).

1.2.1 Total daily insulin dose

From the total daily insulin dose, 40-50% is used overnight, during the fasting period. The other 50-60% is for covering the carbohydrate intake and high glucose blood plasma correction. The daily insulin dose rate is usually constant (Kennedy et al., 2017). Insulin doses are quantified in units of insulin (UI). The total daily insulin requirement (TDI) of a patient is, see equation (1-1).

$$TDI\ [UI] = 0.55 * body\ weight[kg]$$

(1-1)

This can be used as a rule of thumb. Calculation of the basal patient insulin dose will be 50% of the total daily insulin requirement, see equation (1-2). When using an insulin pump, fast-acting insulin can be used at a constant flow rate. Or else long-acting insulin like Glargine or Determir can be administered by an injection.

$$Basal\ insulin\ dose = 0.5 * TDI \tag{1-2}$$

One unit of insulin can cover a certain amount of carbohydrates. The insulin - carbohydrate ratio covers the amount of carbohydrates in grams disposed of per unit of insulin. The sensitivity to insulin varies among patients. Approximately 12-15 grams of carbohydrate will be disposed of when one unit of insulin is administered (Kennedy et al., 2017).

The next calculation shows how much insulin is necessary to cover the carbohydrate intake. See equation (1-3), the carbohydrate insulin coverage dose.

$$M_{cm} = Carbohydrate\ in\ the\ meal\ [g]. \tag{1-3}$$
$$C_{ui} = Carbohydrate\ disposed\ by\ one\ administered\ UI\ [g \cdot UI^{-1}].$$
$$CHO_{icd} = CHO\ disposed\ by\ one\ administered\ UI.$$
$$CHO_{icd} = \frac{M_{cm}}{C_{ui}}$$

1.2.2 Carbohydrate coverage ratio - the rule of 500

Carbohydrate coverage ratio by the rule of 500. See equation (1-4). With this equation, the amount of insulin is determined that is needed for glucose disappearance.

$$CHO\ coverage\ ratio = \frac{500}{TDI} \tag{1-4}$$

When this formula is used, a constant response of the patient body to insulin is assumed. As mentioned before there is a certain fluctuation in patient's insulin sensitivity during the day. Other factors like stress or sports activity will have an influence on insulin sensitivity. So the insulin to carbohydrate ratio may vary daily (Kennedy et al., 2017).

When a high blood glucose is measured, fast-acting insulin is needed. The plasma glucose level decrease will be approximately 50 mg/dL (2.8 mmol/L) to

one unit of insulin. Nevertheless, the range of 15-100 mg/dl to one unit of insulin is possible depending on other factors, like stress, illness and other hormones (Kennedy et al., 2017).

When a high actual blood glucose level, C_{ag} mg/dL is measured, the patient is off target. A correction dose of insulin is needed, which we call the high blood glucose correction dose. The patient has a target blood glucose level, C_{tg} mg/dL (for example 120 mg/dL). It can be calculated how many units of insulin (UI) are needed to get on target again with equation (1-5). As mentioned before, the individual insulin sensitivity factor (ISF) can vary according to the time of the day. The ISF is also known as the patient blood glucose correction factor. The patient needs to know on which part of the day insulin resistance occurs, and likewise, when he is more sensitive to the administered insulin. (Kennedy et al., 2017).

$$I = \frac{C_{ag} - C_{tg}}{ISF}$$ (1-5)

The values found in equations (1-3) and (1-5) are added, resulting in patients total meal insulin dose, I_{tid}, see equation (1-6). This is the amount of insulin the patient should be administering to stay on the target blood glucose level.

$$CHO_{icd} = CHO\ insulin\ coverage\ dose\ [UI]$$ (1-6)
$$I_{hgc} = high\ blood\ glucose\ correction\ dose\ [UI]$$
$$I_{tid} = CHO_{icd} + I_{hgc}$$

1.2.3 High blood sugar correction factor - the rule of 1800

When a high blood glucose level is found by testing the patients' blood, the need for reducing its blood glucose level to target is highly desirable. The next equation (1-7) will give the correction factor of the patients' high blood glucose. After administering insulin, the blood glucose level of the patient will reduce to a certain lower value.

$$correction\ factor = \frac{1800}{TDI}$$ (1-7)

E.g. for a patient with a total daily insulin dose of 40 units of insulin, the correction factor is 45 mg/dL per unit of insulin. This means that when one unit of insulin is administered the blood glucose level will drop by 45 mg/dL.

As mentioned before, all the calculations are rules of thumb. There are many variations of insulin therapy but the stated formulas (1-3) to (1-7) are the initial best guesses for controlling the patients' target blood glucose level (Kennedy et al., 2017).

1.3 Goal

As mentioned in the previous sections, T1DM will ask a lot of the patient's effort to control the BG in euglycemia range. Every time before eating, the following routine starts: cleaning the hands followed by a finger prick, collecting a drop of blood on a test strip for sampling the glucose contents. After counting the CHO content of the meal, the insulin bolus is calculated and injected. After this procedure, the patient can finally eat. After approximate 1.5 – 2 hours, the patient will measure the BG level again, for a possible insulin correction bolus.

To enhance patients' health-related quality of life (HRQoL) an automated artificial pancreas (AP) should be realized. In this way, the BG level is monitored and controlled around the clock with less patient effort resulting in a better HRQoL and a desirable blood glucose level near euglycemia. A basic AP setup will consist of a subcutaneous continuous glucose monitor (CGM), a subcutaneous insulin infusion pump and a control algorithm (Bon, 2013). The core of the AP is the control algorithm.

1.3.1 Research questions

Currently the Dalla Man, Rizza, et al. model is on the cutting edge of T1DM modelling. To validate the model using real patient data, insulin pump data from T1DM patients' is collected in co-operation with the Rijnstate hospital located in the city of Arnhem. The following research questions were set forth:

1. Which information is available to modulate the glucose and insulin kinetics of a human?
2. Which building blocks are needed to build a state of the art T1DM model?
3. Using the patients' and CGM sensor data, is this accurate enough for predicting BG outcome by the state of the art T1DM model?
4. Is it possible to enhance accuracy of the model, by using parameter estimation?

2　Mathematical models of the glucose and insulin system

To find, improve and judge the treatment of TD1M disease, mathematical models describing and explaining the glucose and insulin system are most important. Apart from providing explanations, these models enable prediction of glucose levels in TD1M patients depending on insulin injection and other external and internal factors. This is crucial for the support and monitoring of treatment and ultimately leads to the ability to perform automatic control of insulin injection. The model predictions can be graphically represented to give patients insight into their glucose metabolism. A validated model of sufficient accuracy may replace in vivo tests in the future. Also for the design and evaluation of glucose sensors, a model could be used.

In this section, the base of diabetes modelling is described. The starting point is the model of a normal patient without DM. The glucose disappearance models and insulin kinetics are combined. Every patient will have a metabolic portrait within a certain patient's specific range (persons will react differently on insulin and CHO intake). Later the model of glucose, the model of insulin and the patient's metabolic portrait are combined to make an overall model.

2.1　The minimal modelling approach

Combining an insulin kinetics model and the glucose disappearance model is called the minimal modelling approach by (Pacini & Bergman, 1986), abbreviated to MINMOD. The differential equations of the MINMOD model are (2-1), (2-2) for the glucose disappearance and (2-3) for the insulin kinetics.

$$\frac{dG}{dt} = -X(t) \cdot G(t) + p_1 \cdot \left(G_b - G(t) \right) \tag{2-1}$$

$$\frac{dX}{dt} = -p_2 \cdot X(t) + p_3 \cdot (I(t) - I_b) \tag{2-2}$$

$$\frac{dI}{dt} = -n \cdot I(t) + \gamma \cdot (G(t) - h) \cdot t \tag{2-3}$$

The basal plasma glucose concentration is denoted by G_b with associated unit mg/dL. According to equation (2-1), glucose will enter the plasma compartment when the plasma glucose level $G(t)$ is below the basal plasma glucose level G_b. Glucose will leave the plasma compartment when its level is above G_b. These in

and out fluxes of glucose are proportional to the difference between $G(t)$ and G_b. The insulin activity in the interstitial tissue $X(t)$ will decrease the plasma glucose level (glucose will enter the cell on an insulin stimulus and is converted to energy when needed).

If the insulin level $I(t)$ is above the basal plasma insulin concentration, (denoted by I_b, and associated unit in µU/mL), insulin will enter the interstitial tissue compartment as described by equation (2-2). If the level of insulin falls below I_b, insulin will leave the interstitial tissue compartment.

The glucose effectiveness, S_G equals parameter p_1 in equation (2-1). The ratio p_3/p_2 equals the insulin sensitivity index S_1. S_G and S_1 will be further explained in section 2.2. The fractional insulin clearance parameter is denoted by n in equation (2-3) with an associated unit of min^{-1}. It is also called the insulin disappearance time constant. The glucose threshold level is denoted by h, see equation (2-3). The second phase secretion of insulin Φ_2 (Appendix A) is proportional to γ until the glucose level exceeds the threshold value of h (Bergman, Phillips, & Cobelli, 1981).

Using the MATLAB code and for the input the Frequently Sampled Intravenous Glucose Tolerance (FSIGT) dataset, the MINMOD model is simulated. The model simulation outcome is visualized in Figure 6 and Figure 7. It can be clearly seen in Figure 6 that the model outcome (red line) will follow the trend of the experimental test data, although in the first 10 minutes a lower glucose model outcome is simulated. At approximate 80 minutes, a higher glucose level is simulated by the model.
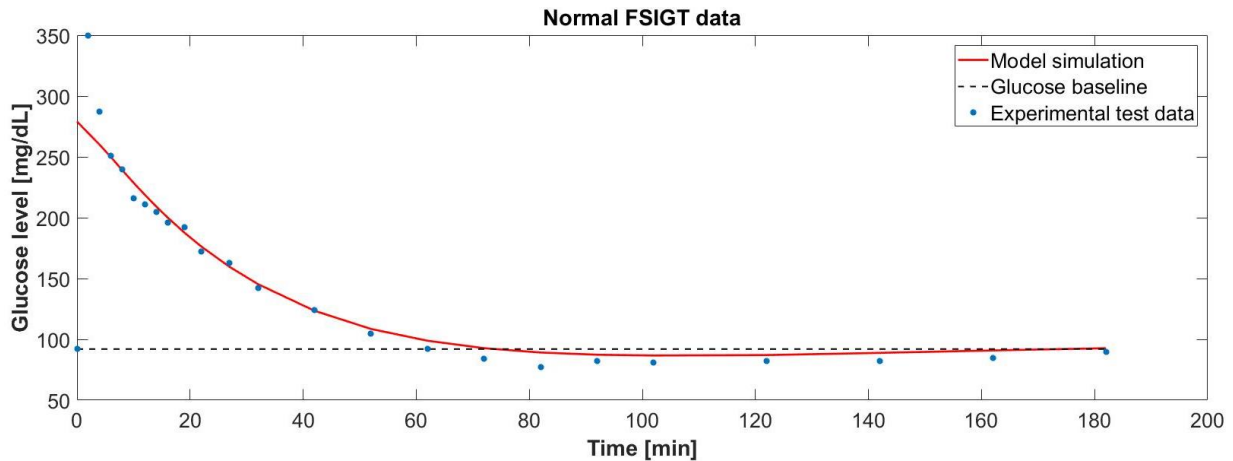
Figure 6.   Minimal modelling approach with normal FSIGT data.

The artificial model compartment of the interstitial insulin X(t) is displayed in Figure 7. Negative influx of insulin at approximate 140 minutes is not representative for humans. In the publication of van Riel (Riel, 2004) the same issue arises.
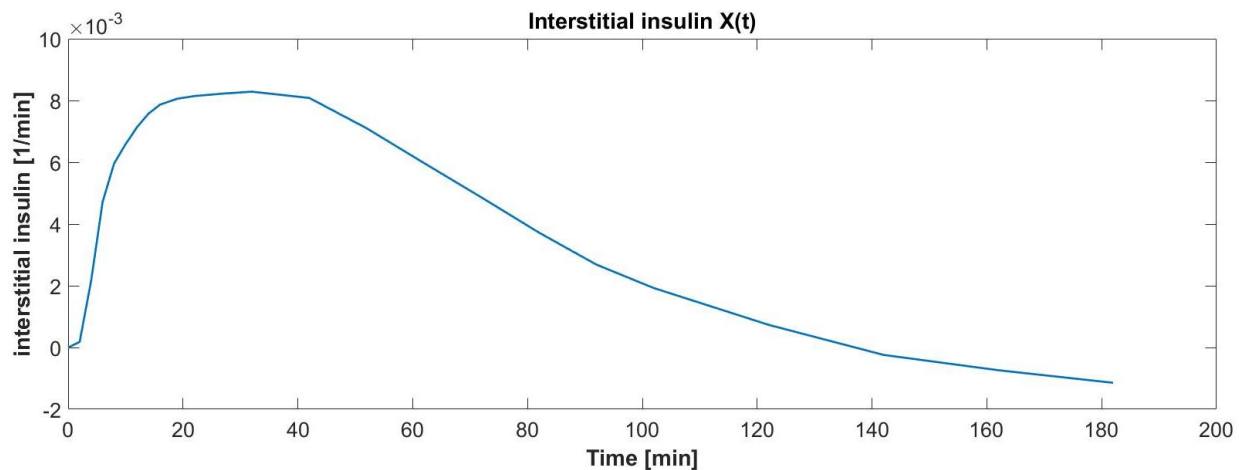
Figure 7.   Interstitial insulin curve from normal FSIGT data.

The model will present a good start for modelling glucose characteristics, but the shortcomings are visible in the figures. The model will not exactly follow the experimental test data plus a negative influx of insulin is not possible.

2.2 Metabolic portrait of an individual

To compute the metabolic portrait of an individual patient, the insulin sensitivity index S_1, equation (2-4), the glucose effectiveness S_G, equation (2-5) and pancreatic responsiveness Φ_1, Φ_2, equation (2-6) are calculated (Bergman et al., 1981). More information about Φ_1, Φ_2 and S_1 is found in Appendix A. The

metabolic portrait is further explained below and relates to the model equations (2-1) and (10-1).

- **Insulin sensitivity (S_1):** the capability of insulin to increase glucose disposal to muscles, liver and adipose tissue.
- **Glucose effectiveness (S_g):** the ability of glucose to enhance its own disposal at basal insulin level.
- **Pancreatic responsiveness (Φ_1, Φ_2):** the ability of the pancreatic β-cells to secrete insulin in response to glucose stimuli. Cited from (Andersen & Højbjerre, 2002, p. 1).

$$S_1 = -\frac{p_3}{p_2} \tag{2-4}$$

$$S_G = p_1 \tag{2-5}$$

$$\phi_1 = \frac{I_{MAX} - I_b}{n \cdot (G_0 - G_b)} \tag{2-6}$$

$$\phi_2 = \gamma * 10^4$$

As mentioned in Appendix A, the hyperglycaemia provokes an excessive release of insulin, see lower panel of Figure 27 located in Appendix A, with the maximum peak value observable at 4 minutes with a value of 130 μU/mL. This maximum insulin peak is called I_{MAX} and used in equation (2-6). The glucose level at t(0) is denoted by G_0 in mg/dL.

2.3 T1DM modelling

For normal glucose disposal in tissue (e.g. no impaired glucose tolerance), three major kinetic processes are needed (Andersen & Højbjerre, 2002). These processes are:

- Tissue needs to be sensitive to insulin
- Glucose could be disposed at a basal insulin level
- β cells of the pancreas secrete insulin to a glucose stimuli

As mentioned before, in a T1DM patient the β cells are defective and no insulin is secreted anymore. To model a patient with T1DM, the insulin secretion related to glucose stimuli needs to be removed from the model equations. Consequently, external insulin input is required.

13

The dynamics of the Bergman's advanced minimal model (Farmer Jr, Edgar, & Peppas, 2009) are described by the following ordinary differential equations (2-7), (2-8) and (2-9). The Bergman's advanced minimal model has been programmed in MATLAB (Saglibene, 2015). The simulation results and parameter values of this model are found in Appendix C.

$$\frac{dG}{dt} = -p_1 \cdot (G(t) - G_b) - G(t) \cdot (X(t) - X_b) + D(t) \tag{2-7}$$

$$\frac{dX}{dt} = -p_2 \cdot (X(t) - X_b) + p_3 \cdot (I(t) - I_b) \tag{2-8}$$

$$\frac{dI}{dt} = -n \cdot I(t) + \frac{U(t)}{V} \tag{2-9}$$

The plasma insulin level is denoted by I, in mU/L, X represents the active insulin in the interstitial space, proportional to the plasma insulin level, in min^{-1}. As mentioned before, X is an artificial model compartment. G represents the plasma glucose in mmol/L. U is the insulin administering input in mU/min. D is the CHO input in mmol/L/min (Saglibene, 2015).

3 Dalla Man model

During an extensive literature survey, see chapter 9, several models are examined. The major limitation of these models is that they are validated only on plasma glucose concentrations. Therefore the physiology of the biochemical phenomena needs to be updated. The next step is to collect information on blood glucose levels in conjunction with the patient's food intake and administering of subcutaneous (exogenous) insulin.

Basu et al. presented a meal dataset of 204 normal individuals in the age of 56±2 years and a body weight of 78±1 kg. From this dataset, the time course of all relevant glucose and insulin fluxes during a meal is obtained (Basu et al., 2003). Next, the dataset is used to develop a meal simulation model of the glucose-insulin system (Dalla Man, Rizza, & Cobelli, 2007). A block diagram of this model is depicted in Figure 8. Simulation results of a normal individual and a T2DM patient are visualized Figure 9 and Figure 10. These figures follow the trend of the model outcome which is presented by Dalla Man, Rizza, et al.
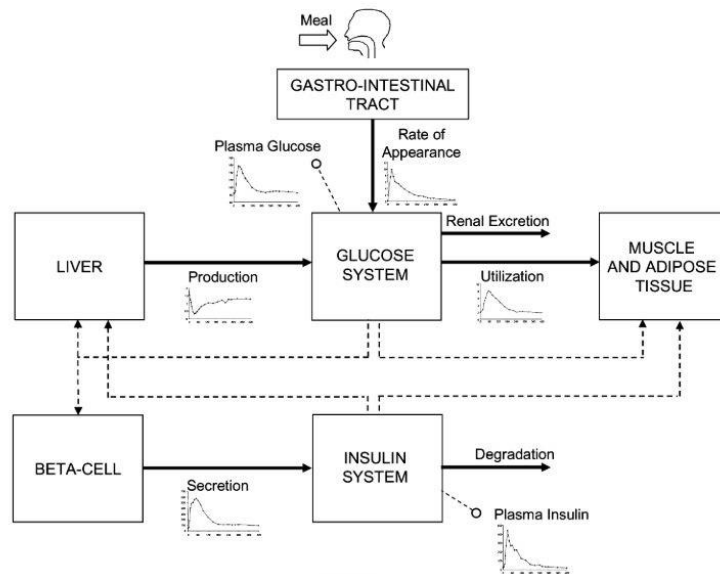
Figure 8.   Scheme of the glucose-insulin control system (Dalla Man, Rizza, et al., 2007).
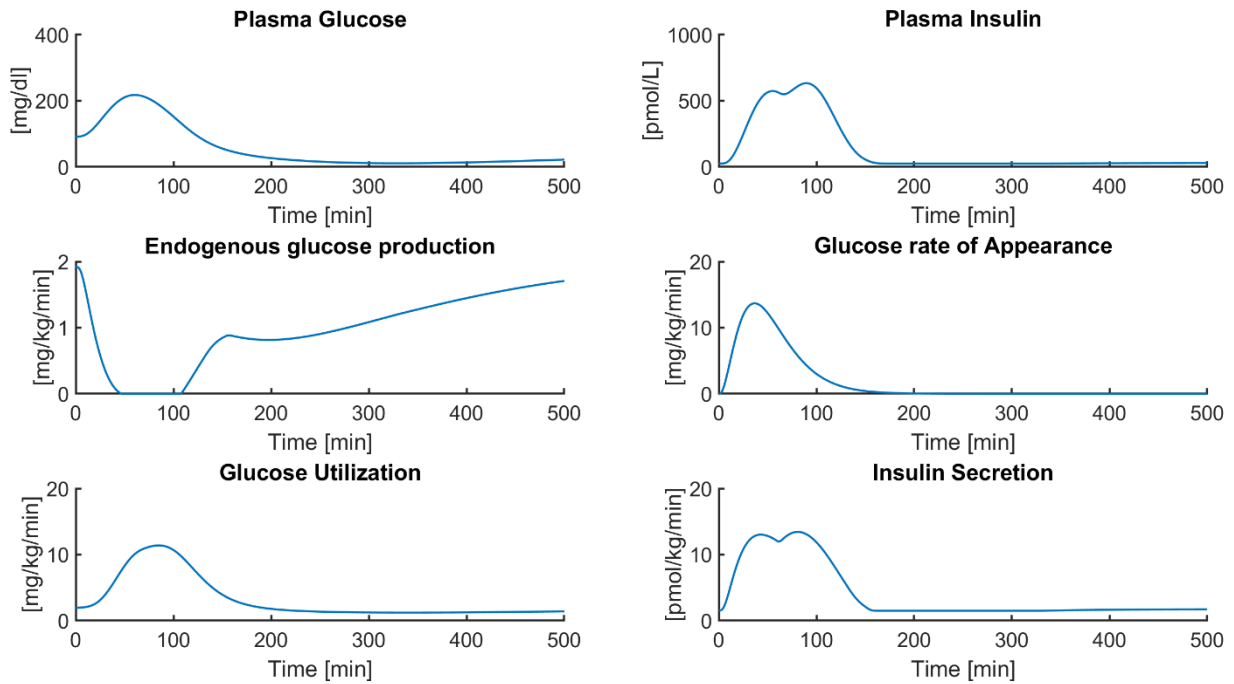
Figure 9. Model simulation of the Glucose-Insulin System using normal patient parameters. The presented results follow the model outcome of Dalla Man, Rizza, et al.
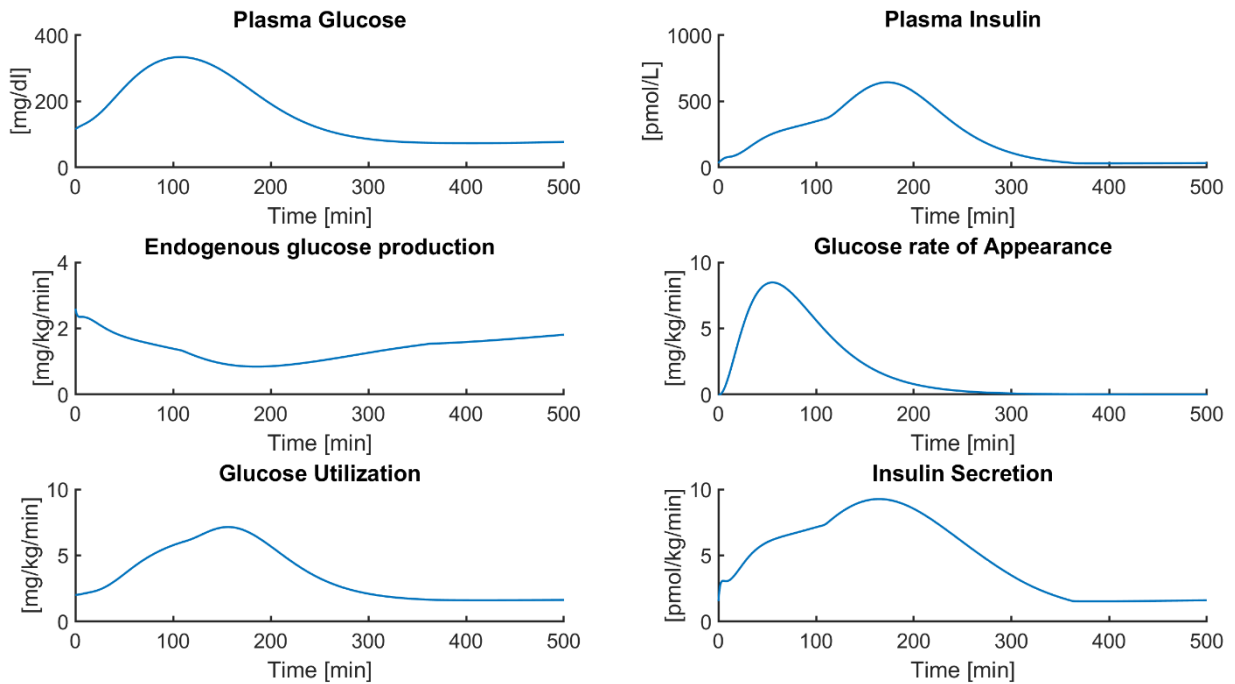
Figure 10. Model simulation of the Glucose-Insulin System using T2DM patient parameters. The presented results follow the model outcome of Dalla Man, Rizza, et al.

During the extensive literature survey a total T1DM model solution was not found. Therefore combining formulas from different publications was the only solution. This is a major contribution to my research to an AP.

The presented Dalla Man model is converted to a T1DM model by combining formulas found in the following literature: The glucose-insulin dynamics from Meal Simulation of the Glucose-Insulin System (Dalla Man, Rizza, et al., 2007), The digestion dynamics of glucose from A System Model of Oral Glucose Absorption: Validation on Gold Standard Data (Dalla Man, Camilleri, & Cobelli, 2006), The subcutaneous insulin administering from GIM, Simulation Software of Meal Glucose-Insulin Model and the UVA/PADOVA Type 1 Diabetes Simulator: New Features (Dalla Man et al., 2014; Dalla Man, Raimondo, Rizza, & Cobelli, 2007).

Using state space methods, the model is implemented in MATLAB. All states, parameters, in- and outputs are listed in the state space mapping table, see Table 1 below.

Table 1.   State space mapping of the Dalla Man, Rizza, et al. model.

State Space Notation	Application Field	Sub Category	Explanation	Unit
x1	$G_p(t)$	*States*	Glucose mass in plasma and rapidly equilibrating tissues	mg/kg
x2	$G_t(t)$		Glucose mass in slowly equilibrating tissues	mg/kg
x3	$I_l(t)$		Insulin mass liver	pmol/kg/min
x4	$I_p(t)$		Insulin mass plasma	pmol/kg/min
x5	$I_d(t)$		Delayed Insulin	pmol/L
x6	$I_{po}(t)$		Amount Insulin in the portal vein	pmol/kg
x7	$I_{one}(t)$		Delayed insulin signal	pmol/L
x8	$Q_{sto1}(t)$		Amount of glucose mass in the stomach	mg
x9	$Q_{sto2}(t)$		Amount of glucose mass in stomach liquid phase	mg
x10	$Q_{gut}(t)$		Amount of glucose mass in the intestine	mg
x11	$X(t)$		Remote insulin	pmol/L
x12	$Y(t)$		Secretion of high plasma glucose	pmol/kg/min
x13	$I_{sc1}(t)$		Nonmonomeric insulin in the subcutaneous space	pmol/kg
x14	$I_{sc2}(t)$		Monomeric insulin in the subcutaneous space	pmol/kg
p1	k_1	*Glucose kinetics*	Rate parameter	1/min
p2	k_2		Rate parameter	1/min
p3	VG		Distribution volume of glucose	dL/kg
p4	m_1	*Insulin kinetics*	Rate parameter	1/min
p5	m_2		Rate parameter	1/min
p6	m_4		Rate parameter	1/min
p7	VL		Distribution volume of insulin	L/kg
p8	m_5		Rate parameter	min kg/pmol
p9	m_6		Rate parameter	unitless

p10	HE_b	*Endogenous Production*	Extraction of insulin	unitless
p11	k_{p1}		Endogenous Production	mg/kg/min
p12	k_{p2}		Liver glucose effectiveness rate parameter	1/min
p13	k_{p3}		Endogenous Production	mg/kg/min/pmol/l
p14	k_{p4}		Endogenous Production	mg/kg/min/pmol/kg
p15	k_i		Endogenous Production rate parameter	1/min
p16	k_{gri}	*Rate of Appearance*	Rate parameter	1/min
p17	a		Rate parameter	1/min
p18	k_{abs}		Rate parameter	1/min
p19	f		The fraction of intestinal absorption which actually happens	unitless
p20	BW		Body weight	kg
p21	k_{max}		Max. emptying rate	1/min
p22	k_{min}		Min. emptying rate	1/min
p23	b		Decrease percentage of k_{empt}	unitless
p24	c		rate maximum	1/mg
p25	d		Increase percentage of k_{empt}	unitless
p26	F_{cns}	*Utilization*	Glucose uptake by brain	mg/kg/min
p27	p_{2u}		Peripheral glucose	1/min
p28	I_b		Basal insulin	pmol/L
p29	V_{m0}	*Michaelis Menten*	Transport rate	mg/kg/min
p30	V_{mx}		Maximum transport rate	mg/kg/min/pmol/L
p31	K_{m0}		Constant for glucose disposal	mg/kg
p32	K_{mx}		Peripheral insulin sensitivity	mg/kg/min
p33	K	*Secretion*	Pancreatic response to glucose rate of change	pmol/kg/ mg/dL
p34	α		The delay between the glucose signal and insulin secretion	1/min
p35	β		Pancreatic responsivity to glucose	pmol/kg/min mg/dL
p36	γ		Transfer rate constant between portal vein and liver	1/min
p37	S_b		Secretion basal rate	pmol/kg/min
p38	k_{e1}	*Renal excretion*	Glomerular filtration rate	1/min
p39	k_{e2}		Renal threshold of glucose	mg/kg
p40	h	*Secretion*	Pancreatic responsivity to glucose	mg/dL
p41	k_d	*Exogenous insulin infusion*	Insulin dissociation	1/min
p42	k_{a1}		Nonmonomeric insulin absorption	1/min
p43	k_{a2}		Monomeric insulin absorption	1/min
d1	D	*Inputs*	CHO food intake	mg
d2	IIR(t)		Exogenous insulin infusion rate	pmol/kg/min
y1	$R_a(t)$	*Outputs*	Glucose rate of appearance	mg/kg/min
y2	G(t)		Plasma glucose concentration	mg/dL
y3	$V_m(X(t))$		Michaelis Menten insulin kinetics	mg/kg/min
y4	$K_m(X(t))$		Michaelis Menten insulin kinetics	mg/kg
y5	$U_{id}(t)$		Insulin dependent utilization	mg/kg/min
y6	E(t)		Glucose renal excretion	mg/kg/min
y7	EGP(t)		Endogenous glucose production	mg/kg/min
y8	S(t)		Insulin secretion	pmol/kg/min
y9	I(t)		Plasma insulin concentration	pmol/L
y10	HE(t)		Hepatic extraction	unitless
y11	$m_3(t)$		Insulin kinetics time-varying parameter	unitless
y12	U(t)		Total glucose utilization	mg/kg/min

3.1 The glucose subsystem of the Dalla Man

The glucose subsystem in Figure 8 consists of two compartments and is depicted in Figure 11. G_p is the glucose mass in plasma, in mg/kg. The total glucose mass in plasma depends on:

- Ra, the rate of glucose appearance from the gastrointestinal tract in mg/kg/min.
- EGP, the endogenous glucose production by the liver in mg/kg/min.
- E, the renal excretion of glucose by the kidneys in mg/kg/min.
- U_{ii}, the insulin-independent glucose utilization by the brain and erythrocytes in mg/kg/min.
- k_1 and k_2, the patient-specific transfer rates in min^{-1}, between the plasma glucose and the glucose mass in the rapidly and slowly equilibrating tissues.

The glucose mass in mg/kg in the slowly equilibrating tissues is denoted by G_t. The total glucose mass G_t, depends on:

- U_{id}, the insulin-dependent utilization by muscle and adipose tissue in mg/kg/min.
- k_1 and k_2 in min^{-1} are the patient-specific transfer rate parameters.
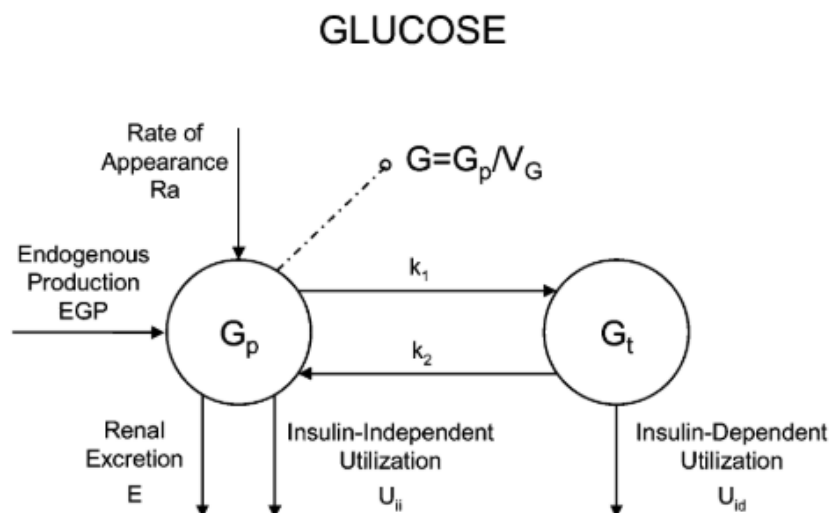
Figure 11. Glucose subsystem (Dalla Man, Rizza, et al., 2007).

The following model equations (3-1), (3-2) and (3-3) define the glucose subsystem. G(t) is the plasma glucose concentration in mg/dL. The distribution volume of glucose is V_G in dL/kg.

$$\frac{dG_p(t)}{dt} = EGP(t) + Ra(t) - U_{ii}(t) - E(t) - k_1 \cdot G_p(t) + k_2 \cdot G_t(t) \qquad \textbf{(3-1)}$$

$$\frac{dG_t(t)}{dt} = -U_{id}(t) + k_1 \cdot G_p(t) - k_2 \cdot G_t(t) \qquad \textbf{(3-2)}$$

$$G(t) = \frac{G_p}{V_G} \qquad \textbf{(3-3)}$$

3.2 The insulin subsystem of the Dalla Man model

The insulin subsystem is depicted in Figure 12 and consists of two compartments. The insulin plasma mass in pmol/kg is denoted by I_p and the liver insulin mass in pmol/kg is denoted by I_l. The distribution volume of insulin is V_I in L/kg. The plasma insulin concentration is denoted by I, pmol/L. The insulin subsystem rate parameters are m_1, m_2 and m_4 in (min^{-1}).
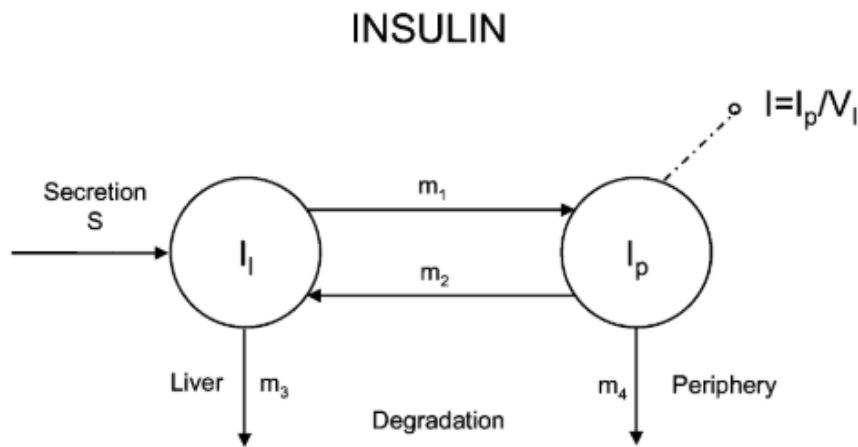
INSULIN

Figure 12. Insulin subsystem (Dalla Man, Rizza, et al., 2007).

A large part of the insulin S(t) (pmol/kg/min) secreted by the pancreas, will be extracted by the liver, m_3(t) and is time-varying. This is described by equations (3-4) and (3-5) and called the hepatic extraction, denoted by HE(t). In steady state, up to 60% of the insulin flux (from the portal vein) is cleared by the liver (Dalla Man, Rizza, et al., 2007). The unit of parameter m_5 is min·kg/pmol and parameter m_6 is unitless.

$$HE(t) = -m_5 \cdot S(t) + m_6 \qquad \textbf{(3-4)}$$

$$m_3(t) = \frac{HE(t) \cdot m_1}{1 - HE(t)}$$

<div align="right">(3-5)</div>

The following model equations (3-6), (3-7) and (3-8) will define the insulin subsystem. I(t) is the plasma insulin concentration in pmol/L and V_l is the distribution volume of insulin in L/kg.

$$\frac{dI_l(t)}{dt} = -\big(m_1 + m_3(t)\big) \cdot I_l(t) + m_2 \cdot I_p(t) + S(t)$$

<div align="right">(3-6)</div>

$$\frac{dI_p(t)}{dt} = -(m_2 + m_4) \cdot I_p(t) + m_1 \cdot I_l(t)$$

<div align="right">(3-7)</div>

$$I(t) = \frac{I_p}{V_l}$$

<div align="right">(3-8)</div>

3.3 Endogenous glucose production

As mentioned before, the blood glucose (G_p) level needs to be as stable as possible. If the G_p is lower than the basal endogenous blood glucose production (EGP_b), the glucagon stimulus will trigger the liver to release more internally stored glucose to keep the blood glucose level as constant as possible. The liver compartment is visualized in Figure 13.

The liver compartment inputs are the glucose and insulin plasma concentration. The endogenous glucose production (EGP) is the liver compartment output.

Figure 13. The liver compartment (Dalla Man, Rizza, et al., 2007).

The following model equations (3-9), (3-10) and (3-11) describe the dynamics of the liver compartment. The extrapolated endogenous glucose production is k_{p1} in mg/kg/min. The liver glucose effectiveness is denoted by k_{p2}, min^{-1}. Insulin action by the liver is denoted by k_{p3} in mg/kg/min per pmol/l. The portal vein insulin action on the liver is denoted by k_{p4}, mg/kg/min per pmol/kg. The delay rate parameter between the insulin signal and insulin action is k_i, min^{-1}. The endogenous glucose production (EGP) is constrained to be non-negative (Dalla Man, Rizza, et al., 2007, p. 1744). $I_{po}(t)$ is the amount of insulin in the portal

vein in pmol/l. I_d (pmol/l) is the delayed insulin signal realised by equations (3-10) and (3-11).

$$EGP(t) = k_{p1} - k_{p2} \cdot G_p(t) - k_{p3} \cdot I_d(t) - k_{p4} \cdot I_{po}(t) \qquad \textbf{(3-9)}$$

$$\frac{dI_1(t)}{dt} = -k_i \cdot \left(I_1(t) - I(t)\right) \qquad \textbf{(3-10)}$$

$$\frac{dI_d(t)}{dt} = -k_i \cdot \left(I_d(t) - I_1(t)\right) \qquad \textbf{(3-11)}$$

3.4 Glucose rate of appearance

The gastrointestinal tract is modelled using three differential equations. Equations (3-13) and (3-14) are used for describing the stomach and (3-15) for describing the gut. The glucose rate of appearance, Ra(t) in mg/kg/min is calculated by using equation (3-16).

Figure 14. The gastrointestinal tract (Dalla Man, Rizza, et al., 2007).

The carbohydrates enter the compartment (Figure 14) and are described by the solid glucose stomach phase, Q_{sto1} (mg). The second phase is the stomach grinding phase (or the glucose liquefying phase) and is indicated by Q_{sto2} (mg). After the glucose is liquefied, the glucose enters the gut. This is the final phase and indicated by Q_{gut} (mg). Equations (3-12)-(3-17) describe the dynamics of the gastrointestinal tract. Parameter k_{gri} is the rate of grinding in min^{-1}. The gastric emptying rate parameter is k_{empt} in min^{-1}. The rate constant of intestinal absorption is k_{abs} in min^{-1}. The CHO food intake, D (mg) is the input to the system. The body weight of the patient in kg is denoted by BW. The fraction of glucose that appears in the blood plasma is denoted by f. For further details about parameters k_{max}, k_{min}, b, d, α and β, refer to a system model of oral glucose absorption (Dalla Man et al., 2006).

$$Q_{sto}(t) = Q_{sto1}(t) + Q_{sto2}(t) \qquad \textbf{(3-12)}$$

$$\frac{dQ_{sto1}(t)}{dt} = -k_{gri} \cdot Q_{sto1}(t) + D \cdot d(t) \tag{3-13}$$

$$\frac{dQ_{sto2}(t)}{dt} = -k_{empt}(Q_{sto}) \cdot Q_{sto2}(t) + k_{gri} \cdot Q_{sto1}(t) \tag{3-14}$$

$$\frac{dQ_{gut}}{dt} = -k_{abs} \cdot Q_{gut}(t) + k_{empt}(Q_{sto}) \cdot Q_{sto2}(t) \tag{3-15}$$

$$Ra(t) = \frac{f \cdot k_{abs} \cdot Q_{gut}(t)}{BW} \tag{3-16}$$

$$k_{empt}(Q_{sto}) = k_{max} + \frac{k_{max} - k_{min}}{2} \cdot \tanh\big(a \cdot (Q_{sto} - b \cdot D)\big) \tag{3-17}$$
$$-\tanh\big(\beta \cdot (Q_{sto} - d \cdot D)\big) + 2$$

3.5 Glucose utilization

The utilization of glucose consists of insulin dependent and insulin independent glucose utilization. The brain and the erythrocytes will utilize the glucose (U_{ii} = F_{cns}) at a constant rate. Thereby the brain and the erythrocytes glucose uptake are the insulin-independent glucose utilization. Muscle and adipose tissue will utilize glucose after an insulin stimulus, so-called the insulin-dependent glucose utilization. Glucose utilization is depicted in Figure 15.
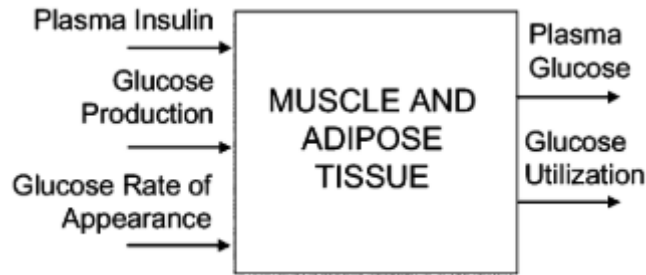
Figure 15. Glucose utilization (Dalla Man, Rizza, et al., 2007).

The glucose-dependent utilization is nonlinear and described with the Michaelis Menten (MM) enzyme kinetics model. For further details about the MM parameters (V_m, K_m, V_{m0}, V_{mx}, K_{m0}, K_{mx}) refer to (Dalla Man, Rizza, et al., 2007). Equations (3-18)-(3-21) describe the dynamics of the glucose utilization compartment. The remote insulin is denoted by $X(t)$ in pmol/l. Insulin-dependent utilization by $U_{id}(t)$ in mg/kg/min. The plasma insulin is denoted by I, suffix b denotes the basal state. Peripheral glucose utilization rate constant is denoted by p_{2U} (min^{-1}).

$$U_{id}(t) = \frac{V_m\big(X(t)\big) \cdot G_t(t)}{K_m\big(X(t)\big) + G_t(t)} \tag{3-18}$$

23

$$V_m\big(X(t)\big) = V_{m0} + V_{mx} \cdot X(t) \qquad \text{(3-19)}$$

$$K_m\big(X(t)\big) = K_{m0} + K_{mx} \cdot X(t) \qquad \text{(3-20)}$$

$$\frac{dX(t)}{dt} = -p_{2U} \cdot X(t) + p_{2U}(I(t) - I_b) \qquad \text{(3-21)}$$

3.6 Glucose renal excretion

If there is no insulin stimulus, the blood glucose level of the patient will rise when CHO is digested. At a certain threshold, the kidneys will excrete the glucose, E(t) into the urine through the kidneys GBM in mg/kg/min. The glucose renal excretion is modelled by equation (3-22). It depends linearly on the blood glucose level.

$$E(t) = \begin{cases} k_{e1} \cdot \big(G_p(t) - k_{e2}\big) & for \ G_p(t) > 0 \\ 0 & for \ G_p(t) \leq 0 \end{cases} \qquad \text{(3-22)}$$

Where k_{e1} (min^{-1}) is the glomerular filtration rate and k_{e2} (mg/kg) is the renal threshold of glucose (Dalla Man, Rizza, et al., 2007).

3.7 Insulin secretion

The insulin secretion by the pancreatic β cells is described by equations (3-23)-(3-25). The insulin secretion compartment is visualized in Figure 16.
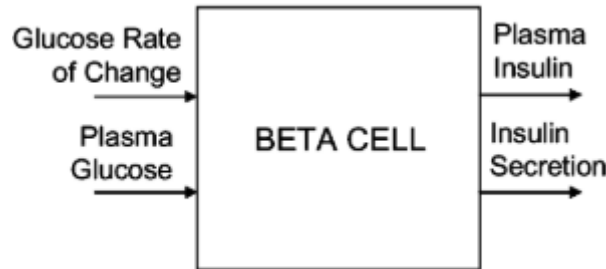
Figure 16. Insulin secretion (Dalla Man, Rizza, et al., 2007).

As mentioned in appendix A, insulin is secreted in two phases. Phase one is the fast insulin secretion which is glucose dependent. The second phase is glucose-independent insulin secretion, at a lower insulin secretion rate. The insulin secretion is denoted by S(t) in pmol/kg/min, the transfer rate (min^{-1}) between portal vein and liver is denoted by γ. Pancreatic responsivity is denoted by K and is in pmol/kg per mg/dl. Secretion of insulin at high plasma level is denoted by Y(t) in pmol/kg/min. For further details about the parameters α, β, and h refer to

meal simulation model of the glucose-insulin system (Dalla Man, Rizza, et al., 2007, p. 1745).

$$S(t) = \gamma \cdot I_{po}(t) \tag{3-23}$$

$$\frac{dI_{po}(t)}{dt} = -\gamma \cdot I_{po}(t) + S_{po}(t) \tag{3-24}$$

$$S_{po}(t) = \begin{cases} Y(t) + K \cdot \dfrac{dG(t)}{dt} + S_b & \text{for } \dfrac{dG}{dt} > 0 \\ Y(t) + S_b & \text{for } \dfrac{dG}{dt} \leq 0 \end{cases}$$

$$\frac{dY(t)}{dt} = \begin{cases} -\alpha \cdot \big(Y(t) - \beta \cdot (G(t) - h)\big) & \text{for } \beta \cdot (G(t) - h) \geq -S_b \\ -\alpha \cdot Y(t) - \alpha \cdot S_b & \text{for } \beta \cdot (G(t) - h) < -S_b \end{cases} \tag{3-25}$$

3.8 Exogenous insulin administering

The subcutaneous insulin kinetics will be used instead of the insulin secretion mode mentioned in chapter 3.7. Through intensive literature survey it was finally found how to transform the Dalla Man, Rizza, et al. model to a T1DM model. A new diagram of the model is presented in Figure 17. The simulated patient is assumed to be in good control, subsequently the rest of the model parameters of the normal patient will be used (Dalla Man, Raimondo, et al., 2007, p. 325; Visentin, Dalla Man, Kovatchev, & Cobelli, 2014). The next equations will describe the T1DM secretion module (Dalla Man et al., 2014). Equation (3-25) will be set to zero when T1DM model simulations are performed.

$$\frac{dI_{sc1}(t)}{dt} = -(k_d + k_{a1}) \cdot I_{sc1}(t) + IIR(t) \tag{3-26}$$

$$\frac{dI_{sc2}(t)}{dt} = k_d \cdot I_{sc1}(t) - k_{a2} \cdot I_{sc2}(t) \tag{3-27}$$

$$R_i(t) = k_{a1} \cdot I_{sc1}(t) + k_{a2} \cdot I_{sc2}(t) \tag{3-28}$$

The amount of nonmonomeric insulin in the subcutaneous space (SCS) is denoted by I_{sc1} in pmol/kg, and the monomeric insulin in the SCS is denoted by I_{sc2} in pmol/kg. The exogenous insulin infusion rate is denoted by IIR(t) in pmol/kg/min. The rate parameters (min^{-1}) of the insulin dissociation, nonmonomeric and monomeric insulin absorption are k_d, k_{a1} and k_{a2}, respectively (Dalla Man, Raimondo, et al., 2007). Finally the insulin delivery rate of appearance in plasma is denoted by $R_i(t)$ in pmol/kg.
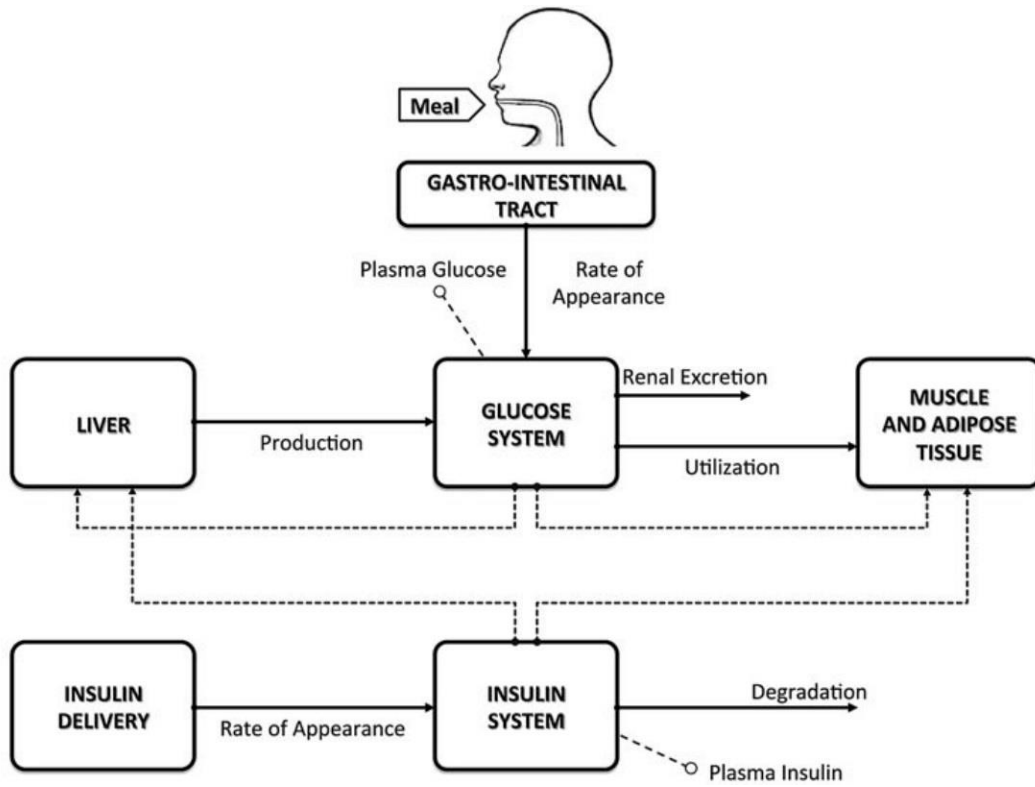
Figure 17. Scheme of the glucose-insulin system with exogenous insulin delivery (Visentin et al., 2014).

4 Patient data

For research purposes and getting hands-on experience, a one-day traineeship at the Rijnstate Paediatric Diabetic Department has been followed. Data is collected from individual patients and is released in accordance with the rules of Rijnstate Hospital Arnhem the Netherlands. Data stored in patients' insulin pumps (for example the Medtronic MiniMed 640G) was extracted and converted for correct data usage in MATLAB. This data is used for estimating certain model parameters, using a nonlinear least squares search method explained in section 5.3.

4.1 Patient data explained

In Figure 18 one-day of T1DM patient data is displayed. The horizontal black lines give an indication of the patients eating time bandwidth during breakfast, lunch and dinner. The numerical values under the horizontal black lines indicate the CHO intake in grams.
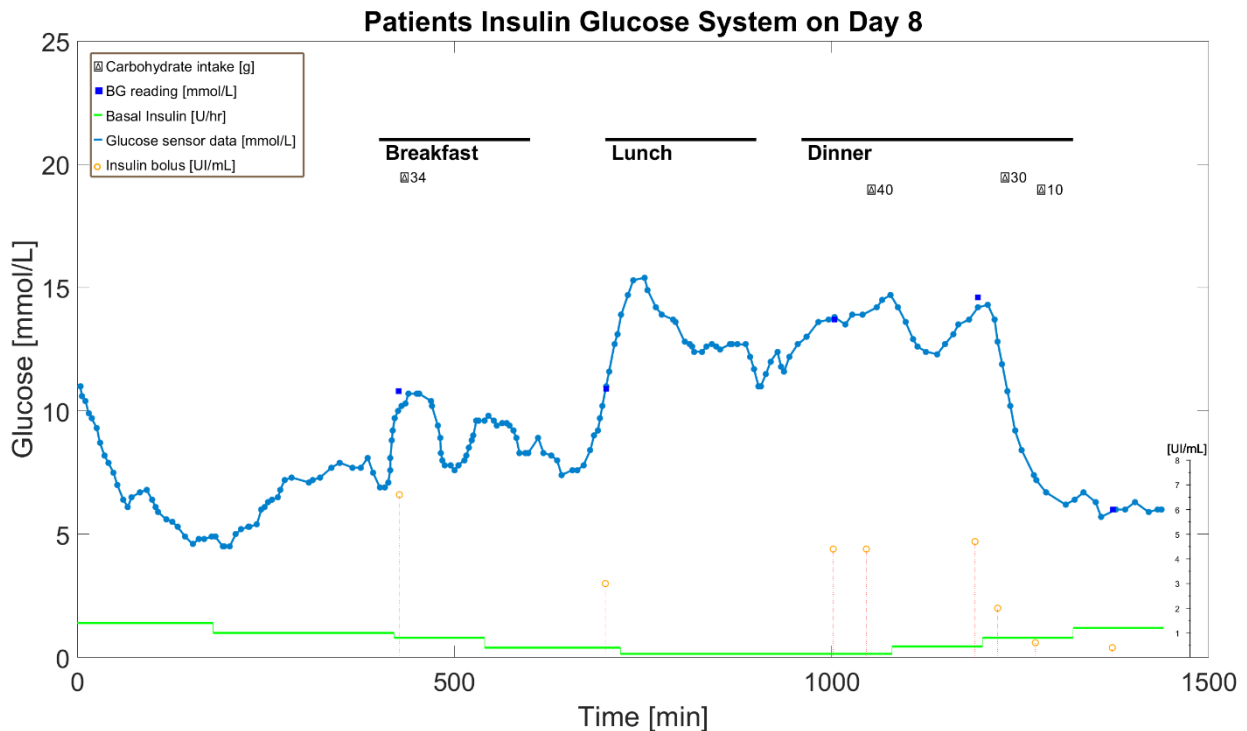
Figure 18. 24-hour T1DM patient data.

The glucose sensor will measure the interstitial glucose level. This sensor data is depicted by the light blue line in the figure in mmol/L. The glucose sensor data is ideal for pattern and trend watching, instead of individual value measurements,

and should not be used for insulin bolus calculation (Medtronic International Trading Sarl™, 2018).

Accurate real-time measurements, for calculating the insulin correction bolus and calibrating the glucose sensor, finger pricks are needed. The blood glucose finger prick measurements in mmol/L are depicted by blue squares in the figure.

The insulin bolus calculation depends on the CHO intake and the blood glucose finger prick measurement and not on the interstitial glucose sensor data as mentioned before. The pump calculates the amount of insulin needed, and delivers it to the patient after patients approval. The insulin correction bolus is depicted as an orange circle in the figure with the corresponding y-axis on the right side.

Because the brain, red blood cells and other tissue will need a consistent basal level of insulin (to keep the vital parts of the human body alive), a constant small delivery of insulin is required by the insulin pump. This is depicted by a horizontal green line: the basal insulin dose, with the corresponding y-axis on the right side.

4.2 Patient data quality

Patient data may be inaccurate. Effort, accuracy and discipline in taking measurements are needed to control T1DM in the euglycemia range. To achieve this, correct carbohydrate information is crucial to calculate the insulin dose correctly. Sometimes patients will lack effort in controlling T1DM, resulting in incorrect data.
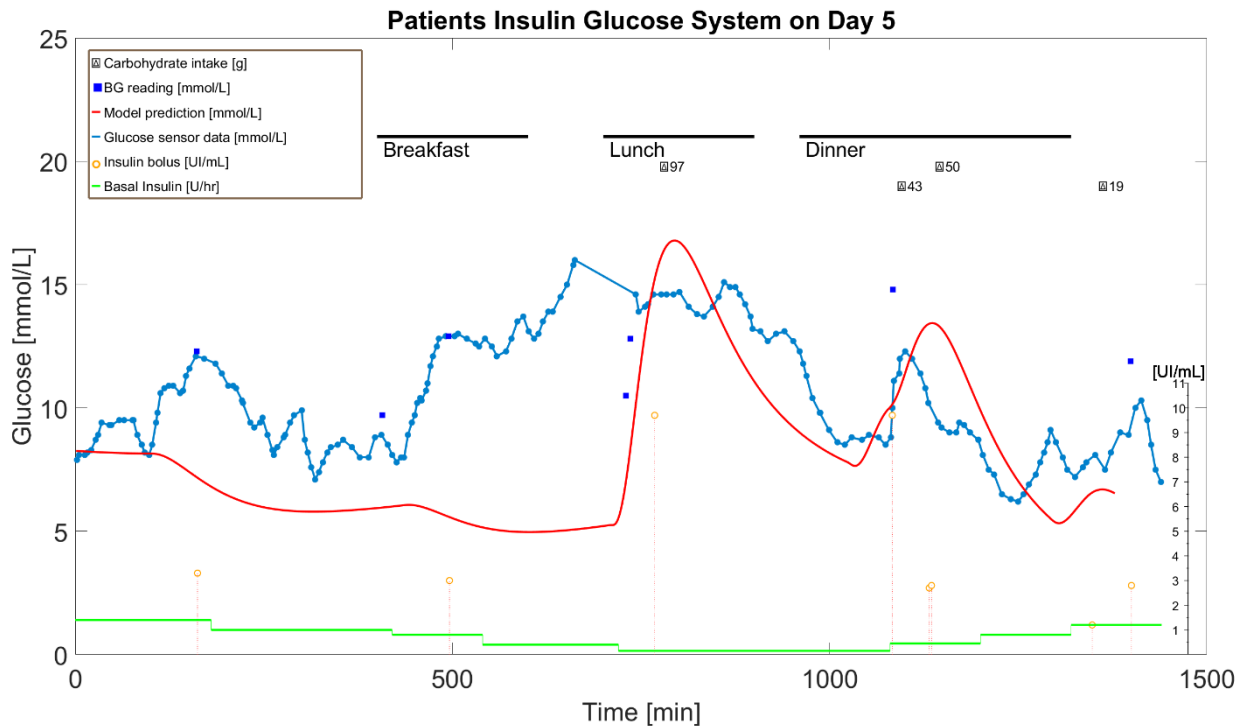
Figure 19. T1DM patient data on day 6 with the model simulation without estimated parameters.

In Figure 19, the model prediction is presented by a red line. From the start of the measurements (time stamp 0 minutes) until approximately midday (700 minutes), there is no correlation between the patient's sensor data and the predicted blood glucose outcome of the model. It can be clearly seen that there are moments of insulin administering and blood glucose finger prick measurements. The assumption is that the patient did not fill the carbohydrate intake in the insulin pump.

As a result of the assumed lack of carbohydrate input until midday and the insulin administering, the simulated blood glucose by the model will decline. Consequently, no correlation is visible between the sensor data and the model outcome. The quality of the patient data is essential for parameter estimation!

4.3 The accuracy of the glucose sensors

Till today the glucose sensors are used for monitoring purposes only (Clarke et al., 2005; Medtronic International Trading Sarl™, 2018). Patients can still not fully rely on continuous glucose sensors. This is because the sensor has a bad accuracy in the hypoglycaemic range (Kropff J. et al., 2015). Furthermore, there is a time lag between the venous blood glucose level (e.g. the finger prick

measurement) and the measured interstitial glucose value by the sensor (Clarke et al., 2005). The mean time lag measured at the abdominal region is 7.94 ± 6.48 min compared to 11.70 ± 6.71 min at the buttocks area for a Medtronic Enlite interstitial fluid glucose sensor (Keenan et al., 2011, p. 225). A time delay can prevent proper estimation of model parameters. A remedy for this is to estimate the time delay too. Figure 20 displays a single patient under cardiac surgery with different glucose measuring devices. In this figure, the differences between arterial blood gas, intravascular microdialysers, subcutaneous measurements, and glucose measurements (point-of-care) can be seen. The intravascular microdialysers CGM (continuous glucose monitor) glucose values followed the reference method (arterial blood gas) very well. The subcutaneous CGM and point-of-care glucometer glucose values also followed the trend of the reference method, although lower glucose values were measured. The Mean Absolute Relative Difference (MARD) (Bon, 2013; Vanstraelen, 2014, p. 7) of this patient was 5.03% for the intravascular microdialysers CGM system, 42.8% for the subcutaneous CGM system, and 17.4% for the point-of-care function of the sensor-reader. (Schierenbeck, Franco-Cereceda, & Liska, 2016).
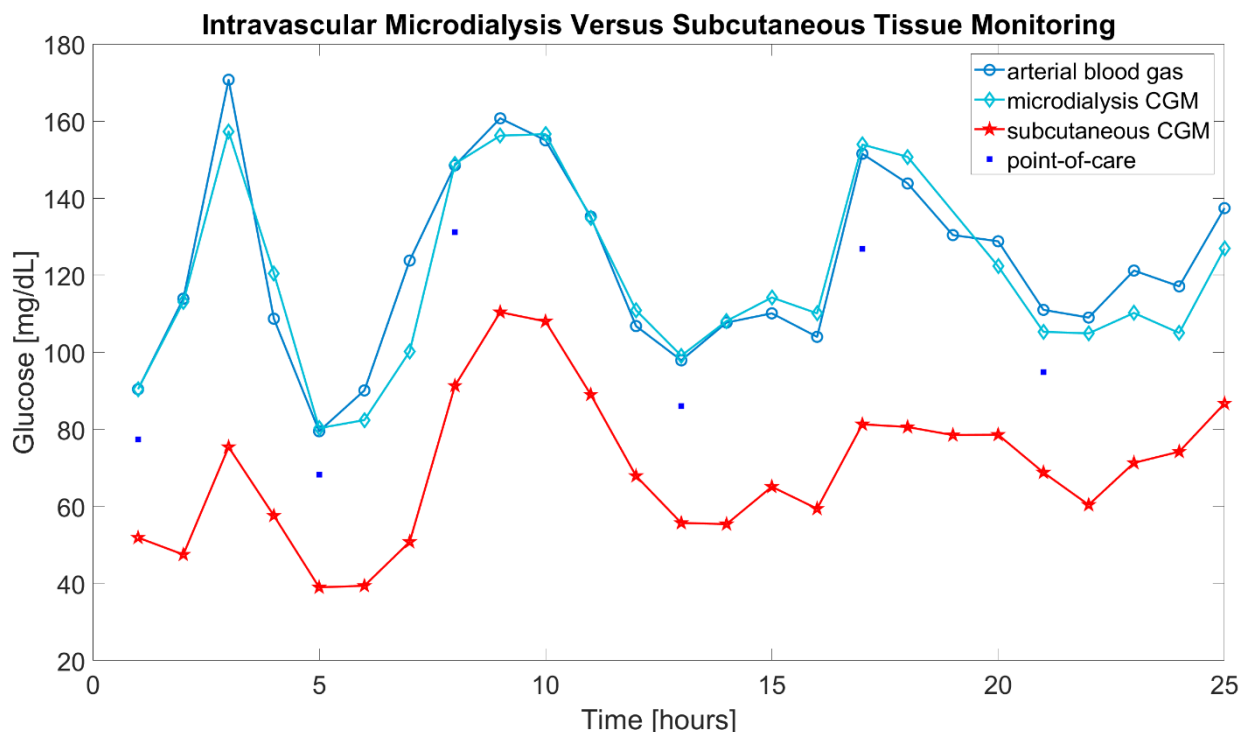
Figure 20. Arterial blood gas analysis vs. microdialysis CGM, subcutaneous CGM and point-of-care (Schierenbeck et al., 2016).

The glucose sensors are evaluated by the International Organization of Standardization (ISO) criteria for blood glucose analysing devices ISO15197:2013. The ISO norm stated that 95% of the readings are ±15% within the reading of the reference value, if this value is above 99 mg/dL (5.5 mmol/L) and ±14 mg/dL (0.78 mmol/L) under 99 mg/dL (5.5 mmol/L) (Schierenbeck et al., 2016).

5 Sensitivity analysis, parameter estimation and model calibration

Model calibration concerns the use of measurement data to estimate unknown or ill-known model parameters to improve model accuracy. Model accuracy benefits most from estimating unknown parameters to which the model is sensitive. To determine this, parameter sensitivity analysis is needed (Briggs et al., 2012; Cohen & van Essen, 1991; van Willigenburg, 2014). When initial state variables are also (partially) unknown, these may also be considered as unknown parameters. After performing parameter sensitivity analysis on a patient model with nominal parameter values, using a dataset (CGM sensor) obtained from a single patient, the most sensitive parameters are estimated resulting in a calibrated model of this patient. Prior to estimating parameters their identifiability is established using a fast algorithm. Identifiability of parameters in a model ensures that they are uniquely determined by the measured data (if model and measurement uncertainty are discarded).

5.1 Sensitivity Analysis

To find out the most sensitive parameters, a parameter sensitivity analysis is necessary (van Willigenburg, 2014). This sensitivity analysis (SA) should be done only on ill-known parameters. Parameters p_{10}, p_{16}, p_{17}, p_{24} and p_{26} are fixed and consequently require no SA. The parameters of the glucose rate of appearance (p_{18}, p_{19}, p_{21} - p_{23} and p_{25}), endogenous glucose production (p_{11} - p_{15}) and glucose utilization (p_{26}, p_{27}-p_{29} and p_{31}) are estimated within precision (Dalla Man, Rizza, et al., 2007). Also, these parameters do not require a SA.

To carry out the SA, a selected parameter value is changed by 5% and after the model simulation from time zero until a final time t_f, the absolute normalized value $\Delta x(t_f)$ of each state variable is recorded. See equation (5-1), where $x_{pert}(t_f)$ is the outcome of the state variable after a parameter change, $x_{nom}(t_f)$ is the nominal outcome and x_{max} the maximum value attainable by that state variable. A low value of $\Delta x(t_f)$ indicates that this state variable of the Dalla Man et al. model is not very sensitive to the selected parameter. If $\Delta x(t_f)$ is significant, the state variable is sensitive to the selected parameter.

$$\Delta x(t_f) = \left| \frac{x_{pert}(t_f) - x_{nom}(t_f)}{x_{max}} \right|$$

A small part of the parameter SA outcome, i.e. values $\Delta x(t_f)$ of a normal individual, are displayed in Figure 21.

State→ Parameter	x1	x2	x3	x4	x5	x6	x7	x8	x9	x10	x11	x12
p1	0,0062	0,0143	0,0247	0,0108	2E-05	0,0188	0,0006	0	0	0	0,0013	0,0246
p2	0,0057	0,0134	0,024	0,0107	4E-05	0,0173	0,0007	0	0	0	0,0016	0,0215
p3	0,0012	0,0018	0,0753	0,0353	0,0001	0,046	0,0027	0	0	0	0,0059	0,0541
p4	6E-05	0,0005	0,0382	0,0076	7E-05	0,0001	0,001	0	0	0	0,0021	0,0002
p5	5E-05	0,0004	0,0101	0,0124	6E-05	1E-04	0,0011	0	0	0	0,0023	3E-05
p6	3E-05	0,0003	0,0067	0,0097	4E-05	5E-05	0,0007	0	0	0	0,0015	1E-04
p7	0,0001	0,0009	0,0001	5E-05	0,0001	0,0002	0,0022	0	0	0	0,0047	0,0004
p8	3E-05	0,0003	0,0298	0,0133	4E-05	5E-05	0,0008	0	0	0	0,0018	0,0002
p9	7E-05	0,0007	0,0672	0,0303	1E-04	0,0001	0,002	0	0	0	0,0044	0,0002
p10	0	0	0	0	0	0	0	0	0	0	0	0
p11	0,0028	0,0022	0,0092	0,0039	9E-06	0,0079	0,0002	0	0	0	0,0005	0,0106
p12	0,0004	0,0003	0,0012	0,0005	1E-06	0,001	3E-05	0	0	0	6E-05	0,0014
p13	0,0002	0,0002	0,0008	0,0003	6E-07	0,0007	2E-05	0	0	0	4E-05	0,0009
p14	0,0011	0,0008	0,0035	0,0014	2E-06	0,0032	7E-05	0	0	0	0,0001	0,0045
p15	3E-06	9E-07	3E-06	9E-07	0,0002	5E-06	0,0019	0	0	0	5E-08	1E-05

Figure 21. Parameter sensitivity analysis, the absolute normalized values $\Delta x(t_f)$ of different state variables for different selected parameters.

From Figure 21 it can be seen that state variables x_2-x_4, x_6 and x_{12} are sensitive to parameters p_1-p_6, p_8 and p_9. This follows from the numbers and corresponding colour bars that are lighted in increasing gradations of red while the grey quadrant indicators are filled proportion wise. Also it can be seen that the sensitivities of state variables x_8-x_{10} are zero. Those states represent food intake. During this parameter SA no food is ingested (model input is zero) so therefore these state values are zero. As mentioned before p_{10} is a fixed parameter value, so SA gives a zero outcome. In appendix D the MATLAB routine used to perform the SA is explained. More results of the SA can be found in Appendix E and Appendix F.

In total 21 runs were conducted with different simulation time lengths, to understand which $\Delta x(t_f)$ responses are observable at the specified end time in conjunction with the changed parameter value.

From the observed data, it can be concluded that the length of simulation time does not have a big influence on the $\Delta x(t_f)$ outcome of the glucose parameters.

During the first 10 minutes, there is at time-delayed response in the insulin kinetics parameters. This is visualized in Table 2 on the next page.

Table 2. Parameters that are sensitive, x indicates multiple sensitive states $\Delta x(t_f)$ at the specified end time. Bold x indicates a higher degree of sensitivity. Red parameters (p_1-p_3) indicate the glucose kinetics, green (p_4-p_9) indicates the insulin kinetics and blue (p_{35}-p_{40}) indicates the insulin secretion kinetics.

Min / Par		1	2	3	4	5	10	15	20	25	30	35	40	45	50	55	60	70	90	100	1440
P_1	k_1			X	**X**	**X**	**X**	**X**	**X**	**X**	**X**	**X**	**X**	**X**	**X**	**X**	**X**	**X**	**X**	**X**	**X**
P_2	k_2	X	X	X	X	**X**	**X**	**X**	**X**	**X**	**X**	**X**	**X**	**X**	**X**	**X**	**X**	**X**	**X**	**X**	**X**
P_3	VG	**X**	**X**	**X**	**X**	**X**	**X**	**X**	**X**	**X**	**X**	**X**	**X**	**X**	**X**	**X**	**X**	**X**	**X**	**X**	**X**
P_4	m_1					X	**X**	**X**	**X**	**X**	**X**	**X**	**X**	**X**	**X**	**X**	**X**	**X**	**X**	**X**	X
P_5	m_2					X	X	X	X	X	X	X	X	X	X	**X**	**X**	**X**	**X**	**X**	X
P_6	m_4						X	X	X	X	X	X	X	X	X	X	X	X	**X**	**X**	X
P_7	VI											X	X	X	X	**X**	**X**	**X**	**X**	**X**	**X**
P_8	m_5				X		**X**	**X**	**X**	**X**	**X**	**X**	**X**	**X**	**X**	**X**	**X**	**X**	**X**	**X**	X
P_9	m_6			X	**X**	**X**	**X**	**X**	**X**	**X**	**X**	**X**	**X**	**X**	**X**	**X**	**X**	**X**	**X**	**X**	**X**
P_{35}	β	**X**	**X**	**X**	**X**	**X**	**X**	**X**	**X**	**X**	**X**	**X**	**X**	**X**	**X**	**X**	**X**	**X**	**X**	**X**	X
P_{36}	γ	X	**X**	**X**	**X**	**X**	**X**	**X**	**X**	**X**	**X**	**X**	**X**	**X**	**X**	**X**	**X**	**X**	**X**	**X**	**X**
P_{37}	S_b				X	X	X	X	X	X	X	X	X	X	X	X	X				
P_{40}	h	X	X	X	X	X	X	X	X	X	X	X	X	X	X	X	X	X	X	X	X

The conclusion is that states x_1-x_4, x_6, and x_{12} are most sensitive to parameter changes. In Table 2, parameters p_1-p_9, and p_{35}-p_{40} appear to be good candidates for parameter estimation. Additional details about the parameters are explained in Table 1.

5.2 Identifiability

Parameters can only be estimated properly if they are locally structural identifiable. Using a fast algorithm (exidghm.m) presented by (Stigter & Molenaar, 2015), we will first check the local structural identifiability of sets of sensitive parameters.

The next parameter vector example is tested for identifiability:
pes = [m_1 m_2 m_4 m_5 m_6 HE_b k_{min} k_{max} V_{m0} V_{mx}]'
The outcome is displayed in Figure 22.
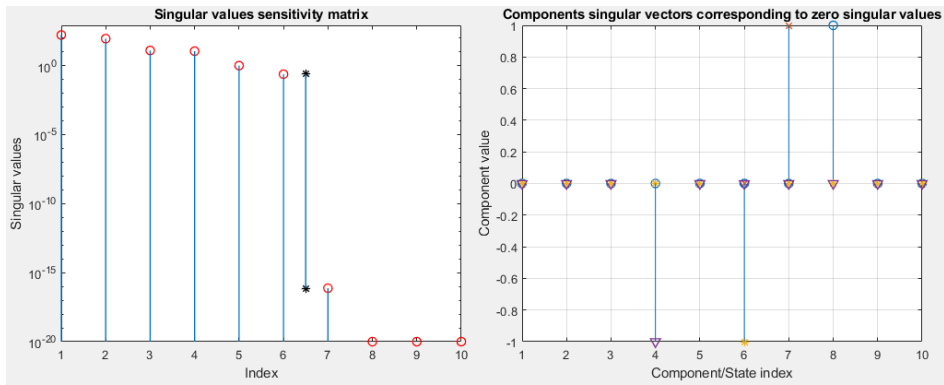
Figure 22. Identifiability of a parameter vector of 10 elements. Parameter 4, 6 – 8 are not identifiable.

It can be seen in the left panel of Figure 22 that a gap is present, distinguished with two black stars, so four of the 10 parameters are not identifiable. From the right panel of the figure the parameters 4, 6, 7 and 8 are not identifiable, respectively: m_5, HE_b, k_{min} and k_{max} in this vector of 10 parameters.
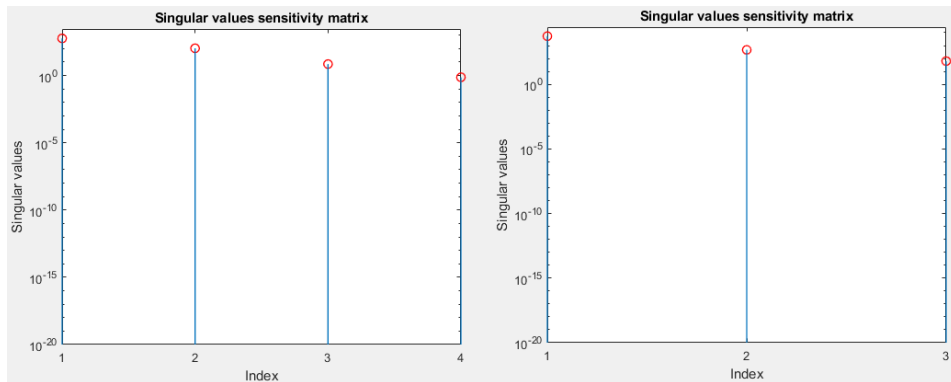
Figure 23. Two parameter sets that are identifiable. No gap present.

Identifiable parameter vectors in Figure 23 (no gap present) pes = [VG k_1 k_2 k_{a1}]' on the left panel, and on the right panel, pes = [VI m_1 m_6]' respectively. Table 3 records the result showing identifiable parameter sets of sensitive model parameters.

Table 3.   Identifiable parameter sets used for calibrating (curve fitting) the model outcome on retrieved patient data.

Set	Parameter			
1	m_2	m_1	m_6	
2	k_{a1}	k_{a2}	k_d	
3	VG	k_1	k_2	k_{a1}
4	k_{a1}	k_{a2}	k_1	k_2
5	VI	m_1	m_6	
6	m_2	m_1	m_6	
7	VI	k_d	k_{a1}	k_{a2}

5.3 Parameter estimation using least squares with patient data

The parameter estimates are obtained from a nonlinear least squares search method represented by Figure 24. (Cohen & van Essen, 1991; van Willigenburg, 2014).
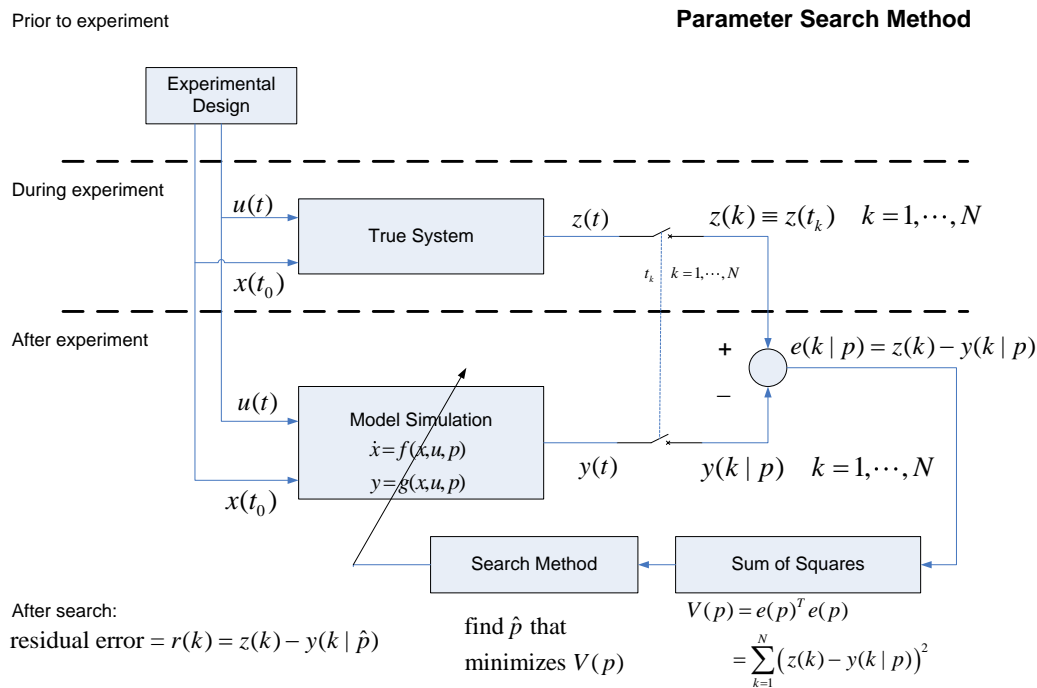
Figure 24. Parameter estimation through minimization of the sum of squared errors. (van Willigenburg, 2014).

By minimizing the sum of squared errors V(p) between the Dalla Man model outcome y(k|p) and measured data z(k) (the observations of the collected patient data and CGM sensor), see Figure 24, parameter estimates collected in the vector $\hat{p}$ are obtained. The search in Figure 24 is performed by MATLAB function 'fminsearch' (Lacouture & Cousineau, 2008; The MathWorks Inc, 2018). In 'fminsearch', the Nelder-Mead algorithm was chosen, because it suffers much less from local minima, caused partly by measurement errors. Using the physical and physiological meaning of model parameters, their search was restricted to a meaningful range. The patient dataset z(k) was obtained from the Rijnstate Hospital Arnhem. As mentioned in section 3.8, the insulin section module (normal patient) will be replaced by the subcutaneous insulin kinetics to transfer the model to a T1DM model. The parameters of subcutaneous insulin kinetics (p_{41}–p_{43}) are used for parameter estimation as well as the parameters (p_1–p_9)

from Table 2. Computations revealed that it is important to also estimate the time-lag of the measurement data to obtain reasonable data fits.

5.4 Result parameter estimation

Results obtained from different parameter estimation runs concerning different parameter sets and datasets from different days are recorded in Table 4. The values in this table equal, formula (5-2).

$$\hat{V}min = \sqrt{\frac{V(p)_{min}}{k(n)}}$$

(5-2)

Formula (5-2), may be loosely interpreted as the average absolute error between the model and measurement data.

Table 4. $\hat{V}min$ **values calculated, using the different patient-data and parameter-sets. Values in green indicate the best optimal fits found.**

Set / Day number	1	2	3	4	5	6	7
1	7.89	7.75	7.54	7.68	7.88	7.89	7.6
2	7.09	6.37	6.30	6.23	6.69	7.09	6.32
3	6.40	5.70	5.10	5.00	6.07	6.40	5.28
4	6.04	5.94	5.92	5.93	6.04	6.04	5.88
5	6.52	5.98	5.96	5.29	6.03	6.52	5.81
6	5.29	4.39	4.71	4.16	4.92	5.29	4.05
7	6.03	6.00	3.44	3.48	3.99	6.03	3.90
8	3.25	3.06	2.30	2.26	2.40	3.25	2.31
9	4.17	3.31	3.34	2.93	3.60	4.17	3.06
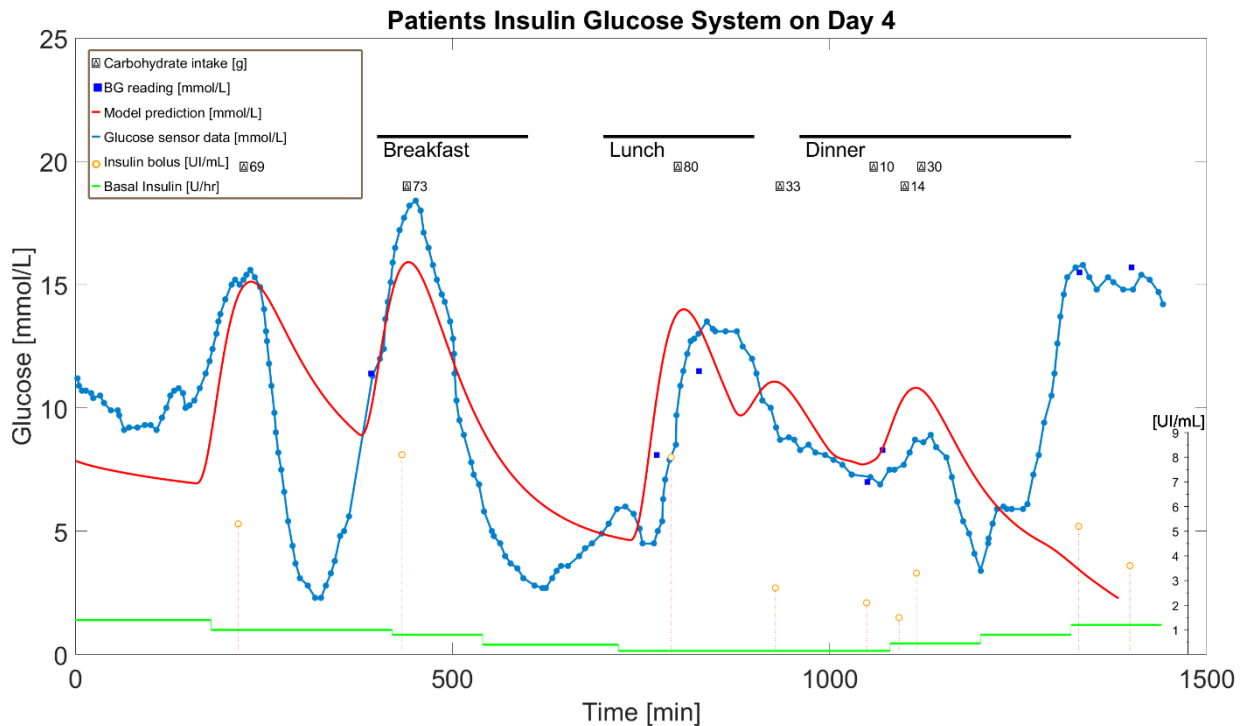
Figure 25. Patient and model outcome simulated on day 4. The Red line is the model simulation outcome using the estimated parameter set 4, with a model time delay of 58 minutes.

In Figure 25, the model outcome will give the best possible fit on the interstitial glucose trajectory of the patient with respect to the CHO intake and administered insulin. The first approximate 1250 minutes the model outcome follows the trend of the CGM. The first and second low glucose levels at approximate 320 and 620 minutes of 2.3 and 2.8 mmol/L respectively are not followed by the model prediction and are in the hypoglycaemia range (≤ 3.8 mmol/L). At around 740 minutes the model prediction is ahead on the CGM. This could be due to the different insulin sensitivities during the day. After 1250 minutes the model outcome is not representative any more. It can be cleary seen that finger pricks are taken and insulin is administered at 1330 and 1400 minutes. Likely, the patient had some late night snack, but no CHO intake was registered in the insulin pump by the patient, resulting in this mismatch in the model outcome.

Using the estimated parameter-set 4 of day 4 on a different day, will give some indication about the quality of the estimated parameter-set 4. This is called cross validation. In Figure 26, parameter set 4 is used for the model simulation of day 10.
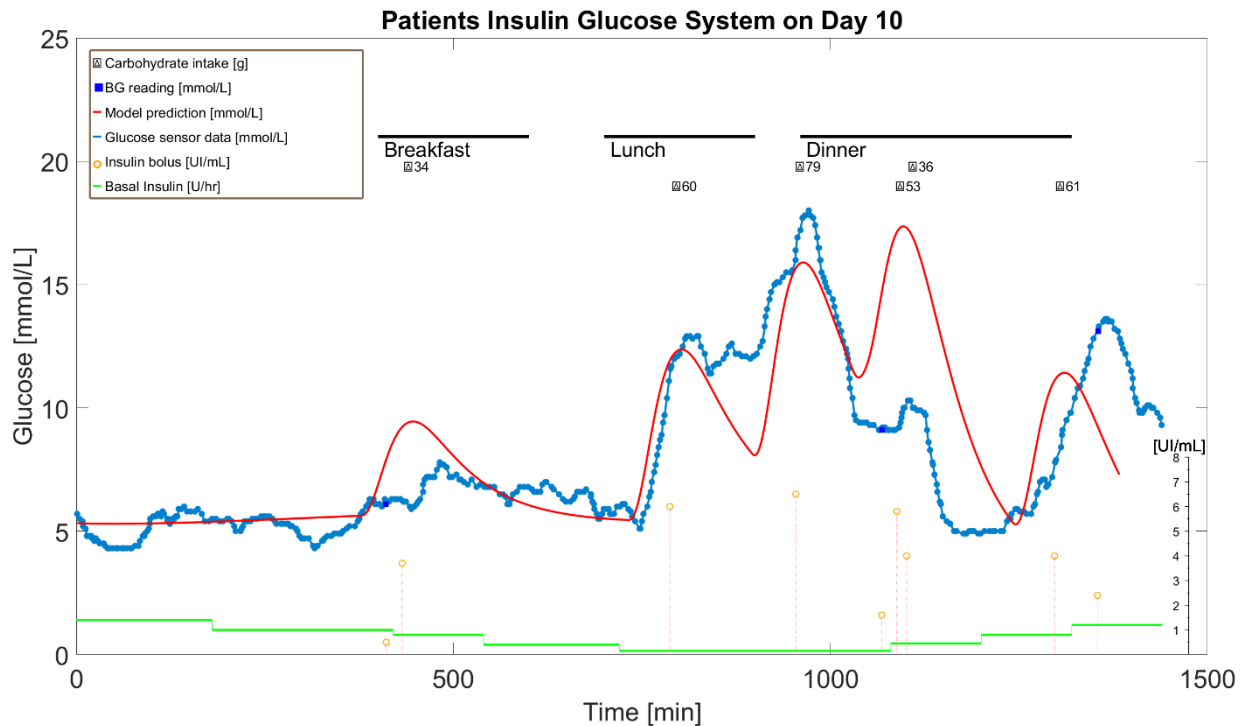
Figure 26. The simulated model outcome of day 10 using the estimated parameter values of set 4.

From Figure 26 it can be seen that no unwanted hypocalcaemia's occur during the day. Around 1070 minutes the patient measures its blood glucose level, and after administering the calculated amount of insulin, the patient will eat something, containing 89 grams of CHO. Comparing the CGM curve with the simulated model outcome the large peak at 1100 minutes of the model outcome is not observable. This model mismatch could again be due to the different insulin sensitivities during the day or an exercise-induced hypoglycaemia (Bon, 2013). An exercise-induced hypoglycaemia will occur during a sports activity when the human body needs more energy than available. A sudden drop in the blood glucose level is then observable.

6   Conclusions

Currently the patients' blood glucose is mostly measured using CGM sensors for the sensor-augmented insulin pump (SAP). The next step is to convert the SAP to an AP (artificial pancreas). Nevertheless a CGM will give the AP an unwanted delayed interstitial glucose level. Therefore a CGM alone is not really suitable for the AP control strategy. From different publications (Kropff J. et al., 2015; Schierenbeck et al., 2016), the arterial blood glucose level is higher than the GCM sensor measured value, in a range of 21.3%. Nevertheless, the CGM will be calibrated on the BG value of the finger prick measurements. This calibration will not remove the delay between blood glucose level and the interstitial glucose level of the patient (Keenan et al., 2011).

Currently mainly CGM sensors are used for registration of the blood glucose. Glucose sensors have a moderate accuracy (shown in Figure 20), and the measured glucose value is lower than the finger prick measurements as mentioned before. From (Schierenbeck et al., 2016) a glucose sensor will have a MARD between 12.0% to 52.1%. A realistic MARD value of an Enlite Medtronic glucose sensor is 21.3% (Vanstraelen, 2014, p. 9).

An artificial pancreas will enhance the HRQoL of the patient. To control T1DM using an AP, the model needs to accurately predict the glucose level and control the exogenous insulin release by the pump. Currently, a lot of input information is needed from the patient to predict the right AP control strategy. Control of T1DM using only patients' CHO intake and CGM data is insufficient in home based situations and could lead to unwanted dangerous situations like coma or even death. Only in the Clinical Research Centre several AP's worked in controlled conditions and with limited CHO intake by the patient (Zisser et al., 2015).

When controlling T1DM using AP model predictions only, unwanted issues arise. For instance unregistered CHO intakes by the patient will result in erroneous model predictions and no exogenous insulin delivery. Thereby the patient's hyperglycaemia range may not match the model predictions as displayed in Figure 25.

Also time-variable parameters are missing in the model, such as different values of the patients' insulin sensitivities during the day. More information on the patients' biomedical reactions is needed. So, more biosensors, with different fields of interest are needed without decreasing the patients HRQoL.

Sports activity and other hormone interactions like stress should be added as model inputs. Also, different types of CHO labelling are required, because different types of carbohydrates will have different effects on the patients' blood glucose fluctuations. Now there is no differentiating between fast and slow carbohydrates. This should be added as an extension in the T1DM model dynamics.

The lack of real-time patient data will result in an insufficient control strategy. The T1DM patient using an AP with only the CGM data and patients' CHO intake patterns as input will lead to inaccurate control. An improved interstitial glucose sensor is first necessary, when thinking about safely controlling an AP in the future, in home based situations.

Overall, T1DM models need to be more accurate in the lower region of the blood glucose level ($\leq$ 3.8mmol/L or 70 mg/dL, (Kropff J. et al., 2015)). Hypoglycaemia is dangerous when no appropriate care is taken. Therefore, models need to react fast and accurately on the signs of a hypoglycaemia. More research is needed in this area to improve the model and the CGM.

A lot of articles and publications about models of DM are present, with the peculiar aspect that minimal information about model calibration is given, and also no real patient data is used to calibrate the T1DM model. Often simulated patient data (data generated by an artificial patient model) is used to compare the T1DM model outcome (Harsh, 2013).

Another odd aspect is that no clear statements are given on how the control algorithm works. Likewise model details are not or only partly described. Nevertheless, these are crucial for a flawless operating AP.

Models suitable for an AP should be calibrated using data from real patients. Rather surprisingly, model calibrations performed in the literature are rare and if performed at all they almost exclusively use data generated by advanced models

rather than data obtained from real patients. Moreover they lack a parameter sensitivity analysis as well as an analysis concerning identifiability of parameter sets. All these are necessary to conduct a proper T1DM model calibration using data from real patients. In this thesis all of these have been successfully performed which is the major contribution of this thesis. Thereby this thesis enables enhancement of the model quality as required for a AP which therefore is not considered a Utopia.

From the sensitivity and identifiability analysis, a selection of parameters is found that is suitable for calibrating the model outcome on patient data. These parameters may be T1DM patient specific, and are divided into three groups: glucose, insulin and exogenous insulin kinetics. The parameter sets suitable for calibration are defined in Table 3.

Finally, after calibrating the model, an independent data set of the same patient is used to compare the model outcome. This is an important, severe test that provides insight into the quality of the model after calibration. Parameter set 4, with the associated parameters of the exogenous insulin kinetics (k_{a1} and k_{a2}) together with the glucose kinetics (k_1 and k_2) gives the best model calibration result. During parameter estimation search bounds are set for the to be estimated parameters. They were set to be ten times bigger and ten times smaller than the nominal parameter value. No parameter clipping was observed. After the parameter estimation, the rate constant parameters of the absorption of insulin (insulin kinetics) has decreased and the rate parameters of the glucose kinetics has increased. The relative changes from the nominal parameter values were as follows: k_{a1} = -0.77, k_{a2} = -0.31 k_1 = 1.15 and k_2 = 1.44 respectively.

The result of the model outcome compared with an independent data set is depicted in Figure 26. This is the first result of the presented T1DM model obtained in this research, having a moderate model accuracy. This accuracy needs to be improved in the future using the procedures developed in this thesis as well as improvements summarized below.

Model improvement should not only be obtained from calibrating the model on specific patient data but also more inputs are needed from the human body. For example an accelerometer, to detect human sport activity, or a sweat detection

sensor that could be used to detect the human stress level (Marques, Silverman, & Sternberg, 2010) could be added. These sensors will provide vital input information to the model of the AP. These two sensors are already on the marked and should be easy implemented in the design of the AP.

An accelerometer will enhance the reduction of a sports induced hypoglycaemia (Bon, 2013). The control system then knows the patient's state of exercise and another control strategy could be chosen by the AP when necessary. A possible exercise-induced hypoglycaemia is present in Figure 26 at about 1100 minutes, and should be detected in the future by the control algorithm.

The patients' stress level will have an effect on the patients' insulin sensitivity. The AP control algorithm can adapt the insulin sensitivity parameter in the future.

Having concluded that an artificial pancreas is not a utopia, the search will continue for an AP in home based situations. With the presented T1DM model and calibrating tools presented in this thesis, a solid basis is formed for further AP model enhancement. Finally the T1DM model simulation outcomes presented in this thesis can also be employed as a learning instrument for patients to better understand the pathogenesis of their disease.

7   Recommendations

The calibration procedures based on data from real patients, as developed and presented in this thesis, should be adopted in future research to enhance the quality of models that are central to an AP.

Accurate (interstitial) glucose and insulin sensors need to be engineered. Today's CGS sensors are not accurate enough (Clarke et al., 2005; Kropff J. et al., 2015; Schierenbeck et al., 2016; Vanstraelen, 2014). Furthermore, the CGS sensor will induce a time lag and is sensor position relevant on the patient's body and patient-specific (Keenan et al., 2011).

In this research, a T1DM model is presented based on the Dalla Man et al. meal simulation model of the glucose and insulin system. The very preliminary outcome is that this model may not be accurate enough to estimate patient glucose levels for an AP. The next step could be, to research the S2008 UVA/PADOVA (Dalla Man et al., 2014), model. It is more extensive than the model presented in this thesis. As mentioned in (Visentin et al., 2014, p. 432) the UVA/PADOVA Type 1 diabetes simulator model will be more accurate because it counter-acts the insulin stimulus by modelling the release of the hormone glucagon. By using the two hormones insulin and glucagon, the AP can control the hyper- and hypoglycaemia range better. When a hypoglycaemia occurs, a glucagon stimulus will release the stored glucose in the liver resulting in a higher BG level. More research on glucagon delivery is required. Subsequently, in the future, an insulin and glucagon delivery pump could be designed as well. And to counteract the limitations of the AP, extended Kalman filtering could be used for AP control (Wang et al., 2014).

8   Useful Abbreviations and Nomenclature

AP	Artificial Pancreas
BG	Blood Glucose
CGM	Continuous Glucose Monitoring
CHO	Carbohydrate
DM	Diabetes Mellitus
FSIGT	Frequently Sampled Intravenous Glucose Tolerance
GBM	Glomerular Basement Membrane
GRS	Glucose Regulatory System
ICD	Implantable Cardioverter Defibrillator
IM	Intramuscular
IV	Intravenous
IVGTT	Intravenous Glucose Tolerance Test
KG	Kinetics of Glucose – Glucose Kinetics
MARD	Mean Absolute Relative Difference
MINMOD	Minimal Model
MM	Michaelis Menten
PP	Pancreatic Polypeptide
SA	Sensitivity Analysis
SAP	Sensor-augmented insulin pump
SCS	Subcutaneous Space
SSE	Sum of Squared Errors
T1DM	Type 1 Diabetes Mellitus
T2DM	Type 2 Diabetes Mellitus
TDI	Total Daily Insulin
HRQoL	Health-Related Quality of Live

9 References

Andersen, K. E., & Højbjerre, M. (2002). A Bayesian approach to Bergman's minimal model. *Insulin, 50*(100), 200.

Atkinson, M. A., Eisenbarth, G. S., & Michels, A. W. (2014). Type 1 diabetes. *The Lancet, 383*(9911), 69-82. doi:10.1016/s0140-6736(13)60591-7

Basu, R., Di Camillo, B., Toffolo, G., Basu, A., Shah, P., Vella, A., . . . Cobelli, C. (2003). Use of a novel triple-tracer approach to assess postprandial glucose metabolism. *American Journal of Physiology-Endocrinology And Metabolism, 284*(1), E55-E69.

Bergman, R. N., Ider, Y. Z., Bowden, C. R., & Cobelli, C. (1979). Quantitative estimation of insulin sensitivity. *American Journal of Physiology-Endocrinology And Metabolism, 236*(6), E667-677.

Bergman, R. N., Phillips, L. S., & Cobelli, C. (1981). Physiologic evaluation of factors controlling glucose tolerance in man: measurement of insulin sensitivity and beta-cell glucose sensitivity from the response to intravenous glucose. *Journal of clinical investigation, 68*(6), 1456.

Bon, A. (2013). *The artificial pancreas, a challenge to research*.

Briggs, A. H., Weinstein, M. C., Fenwick, E. A. L., Karnon, J., Sculpher, M. J., & Paltiel, A. D. (2012). Model Parameter Estimation and Uncertainty: A Report of the ISPOR-SMDM Modeling Good Research Practices Task Force-6. *Value in Health, 15*(6), 835-842. doi:https://doi.org/10.1016/j.jval.2012.04.014

Canadian Diabetes Association. (2017). History of Diabetes. Retrieved from http://www.diabetes.ca/about-diabetes/history-of-diabetes

Clarke, W. L., Anderson, S., Farhy, L., Breton, M., Gonder-Frederick, L., Cox, D., & Kovatchev, B. (2005). Evaluating the clinical accuracy of two continuous glucose sensors using Continuous glucose–error grid analysis. *Diabetes care, 28*(10), 2412-2417.

Cohen, I. R. J., & van Essen, I. N. G. M. (1991). De uitvoering van een praktische identificatie-methode bij gebruik van rekenmodellen voor transport en de distributie van drinkwater.

Dalla Man, C., Camilleri, M., & Cobelli, C. (2006). A system model of oral glucose absorption: validation on gold standard data. *IEEE Transactions on Biomedical Engineering, 53*(12), 2472-2478.

Dalla Man, C., Micheletto, F., Lv, D., Breton, M., Kovatchev, B., & Cobelli, C. (2014). The UVA/PADOVA Type 1 Diabetes Simulator: New Features. *Journal of Diabetes Science and Technology, 8*(1), 26-34. doi:10.1177/1932296813514502

Dalla Man, C., Raimondo, D. M., Rizza, R. A., & Cobelli, C. (2007). GIM, simulation software of meal glucose—insulin model. In: SAGE Publications.

Dalla Man, C., Rizza, R. A., & Cobelli, C. (2007). Meal simulation model of the glucose-insulin system. *IEEE Transactions on Biomedical Engineering, 54*(10), 1740-1749. doi:10.1109/TBME.2007.893506

David Darling. (2016). islets of Langerhans. Retrieved from http://www.daviddarling.info/encyclopedia/I/islets_of_Langerhans.html

Farmer Jr, T. G., Edgar, T. F., & Peppas, N. A. (2009). Effectiveness of intravenous infusion algorithms for glucose control in diabetic patients using different simulation models. *Industrial & engineering chemistry research, 48*(9), 4402-4414.

Gale, E. A. M. (2014). Aretaeus of Cappadocia. doi:https://doi.org/10.14496/dia.1104692125.12

Guyton, A. C., & Hall, J. E. (2006). *Textbook of Medical Physiology* (11th ed.). Philadelphia: Elsevier Sanders.

Harsh, S. (2013). State space modeling and adaptive dual control for Type 1 Diabetes: Evaluation using FDA approved simulator.

Havard T.H. Chan. (2017). Carbohydrates and Blood Sugar. *The Nutrition Source* Retrieved from https://www.hsph.harvard.edu/nutritionsource/carbohydrates/carbohydrates-and-blood-sugar/

Keenan, D., Mastrototaro, J., Zisser, H., A Cooper, K., Gautham, R., W Lee, S., . . . V Shah, R. (2011). *Accuracy of the Enlite 6-Day Glucose Sensor with Guardian and Veo Calibration Algorithms* (Vol. 14).

Kennedy, M. N., Bedrich, M., Gray, L. W., Kroon, L., & Demetsky, M. (2017). Diabetes Education Online, University of California. Retrieved from https://dtc.ucsf.edu/types-of-diabetes/

Kropff J., Bruttomesso D., Doll W., Farret A., Galasso S., Luijf Y. M., . . . DeVries J. H. (2015). Accuracy of two continuous glucose monitoring systems: a head-to-head comparison under clinical research centre and daily life conditions. *Diabetes, Obesity and Metabolism, 17*(4), 343-349. doi:doi:10.1111/dom.12378

Lacouture, Y., & Cousineau, D. (2008). How to use MATLAB to fit the ex-Gaussian and other probability functions to a distribution of response times. *Tutorials in Quantitative Methods for Psychology, 4*(1), 35-45.

Marques, A. H., Silverman, M. N., & Sternberg, E. M. (2010). Evaluation of stress systems by applying noninvasive methodologies: measurements of neuroimmune biomarkers in the sweat, heart rate variability and salivary cortisol. *Neuroimmunomodulation, 17*(3), 205-208.

Medtronic International Trading Sarl™. (2018). Continuous Glucose Monitoring Retrieved from https://www.medtronic-diabetes.co.uk/minimed-system/continuous-glucose-monitoring

Pacini, G., & Bergman, R. N. (1986). MINMOD: a computer program to calculate insulin sensitivity and pancreatic responsivity from the frequently sampled intravenous glucose tolerance test. *Computer Methods and Programs in Biomedicine, 23*(2), 113-122. doi:http://dx.doi.org/10.1016/0169-2607(86)90106-9

Pharma Tips (2013). Human Anatomy & Physiology of Pancreas. Retrieved from http://pharmatips.doyouknow.in/Articles/Human-Anatomy/Human-Anatomy-Physiology-Of-Pancreas.aspx

Riel, N. v. (2004). *Minimal Models for Glucose and Insulin Kinetics - A Matlab implementation -*.

Roberts, J. (2015). Sickening Sweet Retrieved from https://www.chemheritage.org/distillations/magazine/sickening-sweet

Saglibene, M. (2015). *Modelling a type 1 diabetes mellitus patient based on physiological knowledge.*

Schierenbeck, F., Franco-Cereceda, A., & Liska, J. (2016). Accuracy of 2 Different Continuous Glucose Monitoring Systems in Patients Undergoing Cardiac Surgery: Intravascular Microdialysis Versus Subcutaneous Tissue Monitoring. *Journal of Diabetes Science and Technology, 11*(1), 108-116. doi:10.1177/1932296816651632

Stigter, J. D., & Molenaar, J. (2015). A fast algorithm to assess local structural identifiability. *Automatica, 58*, 118-124. doi:10.1016/j.automatica.2015.05.004

The MathWorks Inc. (2018). fminsearch. Retrieved from https://nl.mathworks.com/help/matlab/ref/fminsearch.html

Väisänen, P. (2015). *Modelling Glucose Regulatory System: Adaptive System Dynamic Approach.* (Master of science thesis), Tampere university of technology, Tampere, Finland.

van Willigenburg, L. G. (2014). modelling dynamic systems SCO-20306 lecture notes 1-6 & 7-12.

Vanstraelen, G. (2014). *18 MONTH USE OF MEDTRONIC ENLITE - COMPARISON WITH DEXCOM G4 CGM sensor evaluation*.

Visentin, R., Dalla Man, C., Kovatchev, B., & Cobelli, C. (2014). The University of Virginia/Padova Type 1 Diabetes Simulator Matches the Glucose Traces of a Clinical Trial. *Diabetes Technol Ther, 16*(7), 428-434. doi:10.1089/dia.2013.0377

Wang, Q., Molenaar, P., Harsh, S., Freeman, K., Xie, J., Gold, C., . . . Ulbrecht, J. (2014). Personalized state-space modeling of glucose dynamics for type 1 diabetes using continuously monitored glucose, insulin dose, and meal intake: An extended kalman filter approach. *Journal of Diabetes Science and Technology, 8*(2), 331-345.

Zisser, H., Dassau, E., Lee, J. J., Harvey, R. A., Bevier, W., & Doyle III, F. J. (2015). Clinical results of an automated artificial pancreas using technosphere inhaled insulin to mimic first-phase insulin secretion. *Journal of Diabetes Science and Technology, 9*(3), 564-572.

Inspected publications, but not used for references in this dissertation.

Breton, M., Farret, A., Bruttomesso, D., Anderson, S., Magni, L., Patek, S., . . . Del Favero, S. (2012). Fully integrated artificial pancreas in type 1 diabetes: modular closed-loop glucose control maintains near normoglycemia. *Diabetes*, DB_111445.

Campbell, J. E., & Drucker, D. J. (2015). Islet α cells and glucagon—critical regulators of energy homeostasis. *Nature reviews endocrinology, 11*(6), 329.

Campioni, M., Toffolo, G., Basu, R., Rizza, R. A., & Cobelli, C. (2009). Minimal model assessment of hepatic insulin extraction during an oral test from standard insulin kinetic parameters. *American Journal of Physiology-Endocrinology And Metabolism, 297*(4), E941-E948.

Close, K. (2016). How Does the Oral Glucose Tolerance Test Diagnose Diabetes? Retrieved from https://www.verywell.com/the-oral-glucose-tolerance-test-1087684

Cobelli, C., Dalla Man, C., Toffolo, G., Basu, R., Vella, A., & Rizza, R. (2014). The oral minimal model method. *Diabetes, 63*(4), 1203-1213. doi:10.2337/db13-1198

Cobelli, C., Man, C. D., Sparacino, G., Magni, L., Nicolao, G. D., & Kovatchev, B. P. (2009). Diabetes: Models, Signals, and Control. *IEEE Reviews in Biomedical Engineering, 2*, 54-96. doi:10.1109/rbme.2009.2036073

Colmegna, P., & Sánchez Peña, R. S. (2014). Analysis of three T1DM simulation models for evaluating robust closed-loop controllers. *Computer Methods and Programs in Biomedicine, 113*(1), 371-382. doi:https://doi.org/10.1016/j.cmpb.2013.09.020

Dalla Man, C., Caumo, A., Basu, R., Rizza, R., Toffolo, G., & Cobelli, C. (2004). Minimal model estimation of glucose absorption and insulin sensitivity from oral test: validation with a tracer method. *American Journal of Physiology-Endocrinology And Metabolism, 287*(4), E637-E643.

Dell'Orto, S., Valli, P., & Greco, E. M. (2004). Sensors for rate responsive pacing. *Indian Pacing and Electrophysiology Journal, 4*(3), 137-145.

Dobbins, R. L., Davis, S. N., Neal, D. W., Cobelli, C., Jaspan, J., & Cherrington, A. D. (1995). Compartmental modeling of glucagon kinetics in the conscious dog. *Metabolism, 44*(4), 452-459. doi:https://doi.org/10.1016/0026-0495(95)90051-9

Endmemo. Glucose Unit Conversion.

Fan, K.-Y. D. (2012). Scientific Computing with MATLAB.

Grewal, G. K., & Singh, A. (2011). Molecular Database Generation for Type 2 Diabetes using Computational Science-Bioinformatics' Tools. *International Journal on Computer Science and Engineering, 3*(7), 2811-2817.

Himsworth, H. P. (1949). The syndrome of diabetes mellitus and its causes. *The Lancet, 253*(6551), 465-473.

Hovorka, R. (2006). Continuous glucose monitoring and closed-loop systems. *Diabetic medicine, 23*(1), 1-12.

Ishihara, H., Hashiba, E., Okawa, H., Saito, J., Kasai, T., & Tsubo, T. (2014). Basic and clinical assessment of initial distribution volume of glucose in hemodynamically stable pediatric intensive care patients. *Journal of Intensive Care, 2*(1), 59. doi:10.1186/s40560-014-0059-y

Kaulitzki, S. (2015). The pancreas is located deep inside the abdomen. In.

Kovács, L., Kulcsar, B., György, A., & Benyó, Z. (2011). Robust servo control of a novel type 1 diabetic model. *Optimal Control Applications and Methods, 32*(2), 215-238. doi:10.1002/oca.963

Kovatchev, B. P., Breton, M., Dalla Man, C., & Cobelli, C. (2009). In silico preclinical trials: a proof of concept in closed-loop control of type 1 diabetes. In: SAGE Publications Sage CA: Los Angeles, CA.

Liu, W., & Tang, F. (2008). Modeling a simplified regulatory system of blood glucose at molecular levels. *Journal of Theoretical Biology, 252*(4), 608-620. doi:http://dx.doi.org/10.1016/j.jtbi.2008.02.021

Maas, A. H., Rozendaal, Y. J., van Pul, C., Hilbers, P. A., Cottaar, W. J., Haak, H. R., & van Riel, N. A. (2014). A physiology-based model describing heterogeneity in glucose metabolism: The core of the Eindhoven Diabetes Education Simulator (E-DES). *Journal of Diabetes Science and Technology, 9*(2), 282-292. doi:10.1177/1932296814562607

MacKay, E. M. (1932). The distribution of glucose in human blood. *Journal of Biological Chemistry, 97*, 685-689.

Makroglou, A., Li, J., & Kuang, Y. (2006). Mathematical models and software tools for the glucose-insulin regulatory system and diabetes: an overview. *Applied Numerical Mathematics, 56*(3-4), 559-573. doi:http://dx.doi.org/10.1016/j.apnum.2005.04.023

Mari, A., Pacini, G., Murphy, E., Ludvik, B., & Nolan, J. J. (2001). A model-based method for assessing insulin sensitivity from the oral glucose tolerance test. *Diabetes care, 24*(3), 539-548.

Markakis, M. G., Mitsis, G. D., Papavassilopoulos, G. P., Ioannou, P. A., & Marmarelis, V. Z. (2011). A switching control strategy for the attenuation of blood glucose disturbances. *Optimal Control Applications and Methods, 32*(2), 185-195.

Matsuda, M., & DeFronzo, R. A. (1999). Insulin sensitivity indices obtained from oral glucose tolerance testing: comparison with the euglycemic insulin clamp. *Diabetes care, 22*(9), 1462-1470. doi:10.2337/diacare.22.9.1462

Medtronic. (2018). Diabetes Shop. Retrieved from https://www.diabetes.shop/sensors/enlite/mmt-7008a

Miner, J. H. (2012). The Glomerular Basement Membrane. *Experimental Cell Research, 318*(9), 973-978. doi:10.1016/j.yexcr.2012.02.031

Moler, C. (2013). *Numerical Computing with Matlab*.

Moler, C. B. (2004). *Numerical computing with MATLAB*: SIAM.

Naidu, D. S., Fernando, T., & Fister, K. R. (2011). Optimal control in diabetes. *Optimal Control Applications & Methods, 32*(2), 181-184. doi:10.1002/oca.990

Quiroz, G., Flores-Gutiérrez, C., & Femat, R. (2011). Suboptimal H∞ hyperglycemia control on T1DM accounting biosignals of exercise and nocturnal hypoglycemia. *Optimal Control Applications and Methods, 32*(2), 239-252.

Riel, N. v. (2014a). The Eindhoven Diabetes Education Simulator (e-DES) - incorporating different food products and composite meals In.

Riel, N. v. (2014b). The Eindhoven Diabetes Education Simulator e/DES.

Schiavon, M., Dalla Man, C., Kudva, Y. C., Basu, A., & Cobelli, C. (2014). Quantitative estimation of insulin sensitivity in type 1 diabetic subjects wearing a sensor-augmented insulin pump. *Diabetes care, 37*(5), 1216-1223. doi:10.2337/dc13-1120

Ståhl, F., & Johansson, R. (2009). Diabetes mellitus modeling and short-term prediction based on blood glucose measurements. *Mathematical Biosciences, 217*(2), 101-117. doi:http://dx.doi.org/10.1016/j.mbs.2008.10.008

Thabit, H., & Hovorka, R. (2016). Coming of age: the artificial pancreas for type 1 diabetes. *Diabetologia, 59*(9), 1795-1805. doi:10.1007/s00125-016-4022-4

Visentin, R., Dalla Man, C., Kovatchev, B., & Cobelli, C. (2014). The University of Virginia/Padova Type 1 Diabetes Simulator Matches the Glucose Traces of a Clinical Trial. *Diabetes Technol Ther, 16*(7), 428-434. doi:10.1089/dia.2013.0377

Wisse, B. (2015). Glucose tolerance test - non-pregnant. Retrieved from http://umm.edu/health/medical/ency/articles/glucose-tolerance-test

10 Appendices

A. Bergman minimal glucose model

Bergman (Bergman, Ider, Bowden, & Cobelli, 1979) evaluated seven glucose mathematical models to estimate insulin sensitivity. A catheter was placed through the jugular vein into the right atrium of dogs and an intravenous glucose tolerance test (IVGTT) was performed. From the obtained data, glucose-disappearance, as well as pancreatic insulin release curves, ware made. The insulin data set is later used as the input for the system models. The output of the models is the plasma glucose disappearance. Berman et al. proposed the seven models and after comparison, Bergman concluded that they found meaningful parameter estimates for model VI. Model VI was adopted as the ideal glucose kinetics (KG) model to estimate insulin sensitivity in those days, see Figure 28. This Bergman's model VI is frequently used as the basis for further model development (Väisänen, 2015).

Gathering glucose and insulin data

After fasting period a glucose injection to an animal or man is given. Blood is frequently sampled and after centrifugation the blood sample, the plasma is analysed by a laboratory to reveal the glucose and insulin levels at specified sample time. From this frequently sampled intravenous glucose tolerance (FSIGT) data (Pacini & Bergman, 1986), the dynamic response of pancreatic β cell insulin release and glucose disappearance are found for that specific subject. An FSIGT data file is presented in Appendix B. A MATLAB script is used for the simulation of the minimal KG model, developed by van Riel (Riel, 2004). With minor modifications for better graphical output results, the FSIGT is visualized, see Figure 27.
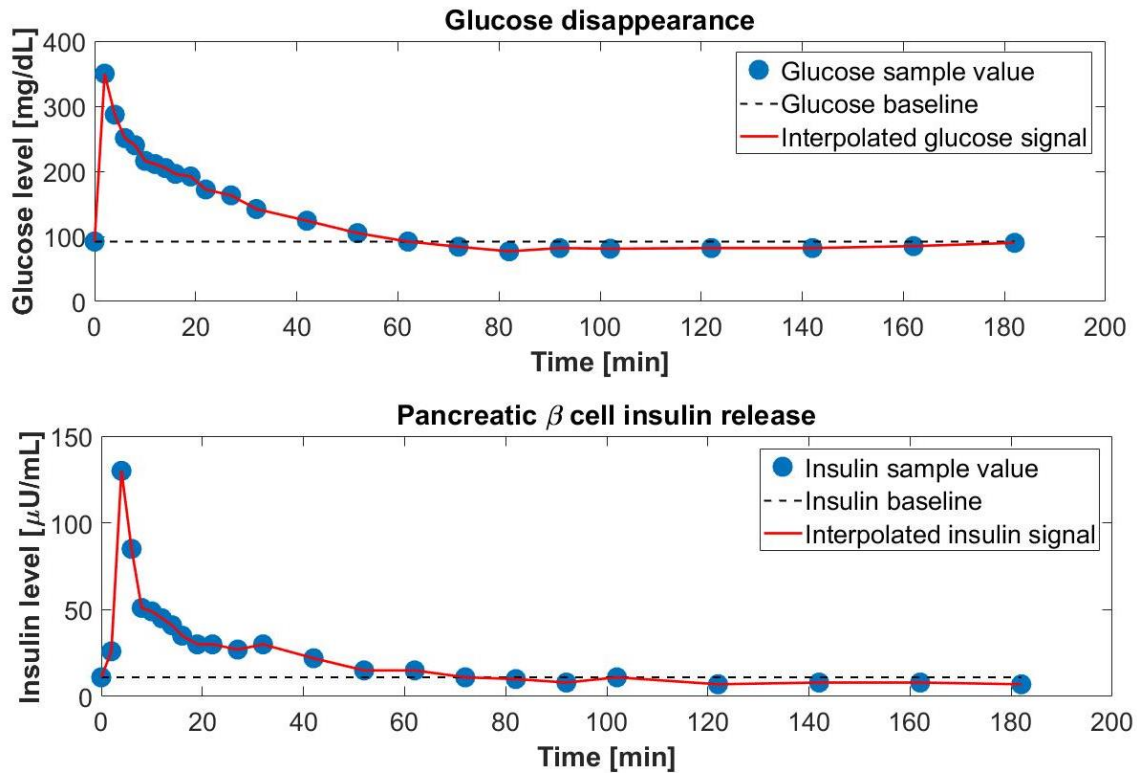
Figure 27. Frequently sampled intravenous glucose tolerance data-set, visualized.

An FSIGT (or IVGTT with frequent sampling) starts with a smooth glucose injection in an antecubital vein, with a duration of 60 seconds and a mass of 300 mg/kg glucose at time $t = 0$ after an overnight fast. The sample duration of the IVGTT is 182 minutes (Bergman et al., 1981). From the obtained data, a typical shape is depicted in Figure 27. After injecting the glucose, hyperglycaemia occurs. A large glucose peak (350 mg/dL) is observable after 2 minutes. In the next 60 minutes after the injection, the plasma glucose level will decrease to the normal baseline plasma glucose level of approximate 92 mg/dL or 5 mmol/L.

The hyperglycaemia provokes an excessive release of insulin, with the maximum peak value observable at 4 minutes (130 μU/mL). In literature (Bergman et al., 1981) this release of insulin is called the *first phase Φ_1*. The second release of insulin, at a lower secretion rate (note, a slower decline in the plasma insulin level) is noticeable and called the *second phase Φ_2*. The two insulin release phases Φ_1 and Φ_2 are caused by the response of the β cells to glucose. Φ_1 and Φ_2 together with the patient's insulin sensitivity (S_1), will form the integrated metabolic portrait of that particular patient (Bergman et al., 1981; Pacini & Bergman, 1986).

Bergman's model VI setup

The blood glucose level in this model is defined as an output of the physiological system. From the patient IVGTT data set, the insulin time course is defined as the input to the system (Bergman et al., 1979). The Bergman's model figure is depicted in Figure 28. The ordinary differential equations for the KG are presented in equations (10-1) and (10-2).

$$\frac{dG}{dt} = (p_1 - X(t)) \cdot G(t) + p_4 \tag{10-1}$$

$$\frac{dX}{dt} = p_2 \cdot X(t) + p_3 \cdot I(t) \tag{10-2}$$
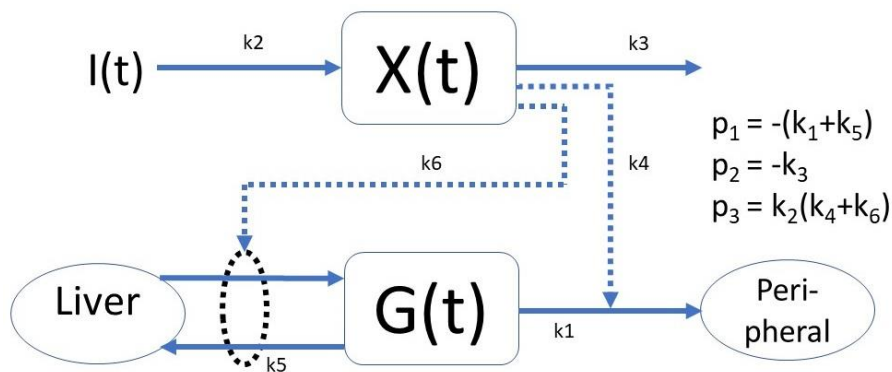
Figure 28. Glucose kinetics model VI (Bergman et al., 1979)

The blood plasma glucose concentration in mg/dL is represented by $G(t)$. The plasma glucose rate of change over time is represented by dG/dt. The remote insulin compartment is represented by $X(t)$. This remote insulin compartment is related to tissue cells that will respond to an insulin stimulus. These tissue cells are also called insulin bounding peripheral tissue and increases the glucose disappearance linear, min^{-1}, after an insulin stimulus. $I(t)$ is the blood plasma insulin input concentration in µU/mL, formed from the FSIGT data set. The independent model variable t is the time in minutes.

The glucose disappearance (the ability of the cells to convert glucose to energy and by an insulin stimulus that results in a glucose uptake by the cells) is encouraged by insulin concentration $I(t)$ through the second term on the right in equation (10-2). The glucose production and glucose uptake by the liver is

grouped together. A net liver glucose balance is modelled (Bergman et al., 1979).

In addition, the Bergman's minimal model estimated parameter values, matching the FSIGT dataset, are found in Table 5.

Table 5. **Model VI parameter values (Bergman et al., 1979)**

p_1	p_2	p_3	p_4
-4.90	-9.10	8.96	4.42
$\pm 0.97 \times 10^{-2}$	$\pm 1.20 \times 10^{-2}$	$\pm 1.88 \times 10^{-5}$	± 0.74

B. Frequently sampled intravenous glucose tolerance data set

Glucose injection, 0.3 g/kg at time t = 0 lasting for 60 s (Pacini & Bergman, 1986, p. 118).

T = time [minutes] G = glucose level [mg/dl] I = insulin level [µU/ml]

T	G	I	T	G	I
0	92	11	32	142	30
2	350	26	42	124	22
4	287	130	52	105	15
6	251	85	62	92	15
8	240	51	72	84	11
10	216	49	82	77	10
12	211	45	92	82	8
14	205	41	102	81	11
16	196	35	122	82	7
19	192	30	142	82	8
22	172	30	162	85	8
27	163	27	182	90	7

C. Simulation result Bergman model and parameter values

The stated figures below are found in the thesis report of Saglibene (Saglibene, 2015, p. 10).
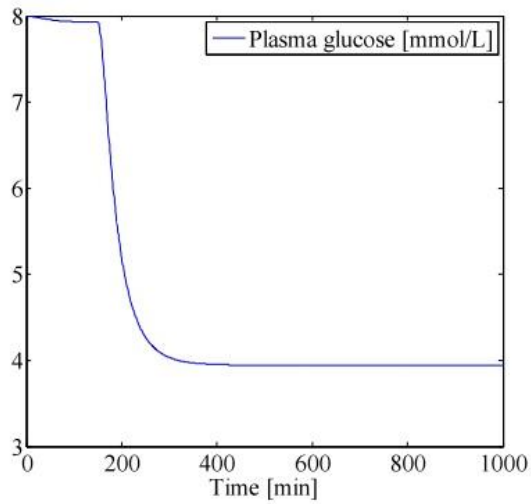
Figure 2. Bergman model response to an insulin bolus of $3\,U$ at $t = 150\,min$.
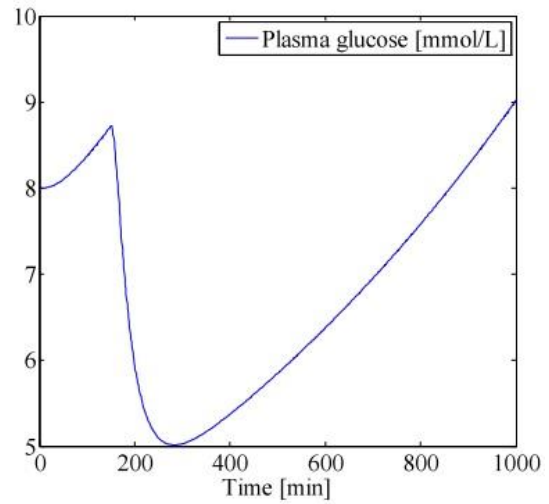
Figure 3. Bergman-basal model response to an insulin bolus of $3\,U$ at $t = 150\,min$.

The stated table below from thesis report of Saglibene (Saglibene, 2015, p. 8).

Parameter	Default value	Unit
p_1	0	min^{-1}
p_2	0.025	min^{-1}
p_3	0.000\,013	$L \cdot mU^{-1} \cdot min^{-2}$
n	0.093	min^{-1}
V	12.0	L
G_b	4.5	$mmol \cdot L^{-1}$
X_b	0	min^{-1}
I_b	15	$mU \cdot L^{-1}$

D. Sensitivity analysis

The parameters and states of the T1DM model are increased with 5%. In this T1DM model, there are 12 states and 40 parameters. This requires 53 model simulations. One model simulation with the nominal parameters and initial state

```
A=[x0 p];                % Initial states and parameter vector
Adelta=A*(per/100);      % Percentage of change in states and parameters
B=ones(nx+np);
C=B*diag(A,0);           % fill matrix with initial states and parameter values
N=C+diag(Adelta,0);      % Add the percentage of change to the states and parameters

M=[A;N];                 % First row of matrix M: the nominal values of the model
```

variables and 52 modified ones.

$\Delta x\left(t_f\right) = x_{pert}\left(t_f\right) - x_{nom}\left(t_f\right)$ is calculated

It is essential to know the behaviour of all the states after an impulse, as described in the introduction. This state information is visualized and will tell for example, how stable the states after a perturbation are and how sensitive the states are to a change. As well as the trajectory of the state response. For example to depict when a steady state occurs.

To visualize the behaviour of all the states for analysing the state behaviour, one master figure is made. In this master figure for every state, one subplot is made. In Appendix, F the total overview of the master figures are included.

As mentioned before 52 simulations are performed, one MATLAB simulation duration costs 4300 seconds (for a 24-hour model simulation) so a sensitivity analysis it is a time-consuming procedure.

E. Sensitivity analysis of a normal patient

Simulation time length of 1 minute

	x1	x2	x3	x4	x5	x6	x7	x8	x9	x10	x11	x12
x1	0,016223	0,002343	0,002292	0,000236	1,75E-09	0,02066	7,2E-07	0	0	0	1,72E-06	0,061146
x2	0,000939	0,027069	0,001857	0,000215	1,8E-09	0,012606	7,06E-07	0	0	0	1,69E-06	0,003535
x3	2,52E-09	2,7E-07	0,003381	0,000978	2,76E-08	7,57E-10	6,59E-06	0	0	0	1,57E-05	9,46E-09
x4	1,56E-08	1,26E-06	0,000397	0,001319	1,3E-07	5,77E-09	2,04E-05	0	0	0	4,84E-05	5,87E-08
x5	2,22E-05	1,59E-06	1,1E-06	8,5E-08	0,005105	1,5E-05	2,02E-10	0	0	0	4,83E-10	8,36E-05
x6	1,45E-05	1,15E-06	0,001237	0,000193	2,58E-09	0,005037	8,29E-07	0	0	0	1,98E-06	5,47E-05
x7	8,86E-08	4,24E-09	2,26E-09	1,42E-10	4,03E-05	4,13E-08	0,003498	0	0	0	6,6E-13	3,33E-07
x8	0	0	0	0	0	0	0	0	0	0	0	0
x9	0	0	0	0	0	0	0	0	0	0	0	0
x10	0	0	0	0	0	0	0	0	0	0	0	0
x11	0	0	0	0	0	0	0	0	0	0	0	0
x12	0	0	0	0	0	0	0	0	0	0	0	0
p1	0,001	0,0023	5E-05	4E-06	2E-11	0,0007	1E-08	0	0	0	2E-08	0,0039
p2	0,0009	0,0022	0,0019	0,0002	2E-09	0,0126	7E-07	0	0	0	2E-06	0,0035
p3	2E-05	1E-06	0,0022	0,0002	2E-09	0,0204	7E-07	0	0	0	2E-06	0,062
p4	3E-09	3E-07	0,0018	0,0011	3E-08	8E-10	7E-06	0	0	0	2E-05	1E-08
p5	2E-09	2E-07	0,0005	0,0008	2E-08	6E-10	5E-06	0	0	0	1E-05	7E-09
p6	8E-10	9E-08	5E-05	0,0004	9E-09	2E-10	2E-06	0	0	0	5E-06	3E-09
p7	2E-08	1E-06	3E-10	1E-11	2E-07	6E-09	3E-05	0	0	0	6E-05	7E-08
p8	4E-11	5E-09	0,0004	5E-05	6E-10	9E-12	2E-07	0	0	0	5E-07	1E-10
p9	4E-10	5E-08	0,003	0,0004	6E-09	1E-10	2E-06	0	0	0	4E-06	2E-09
p10	0	0	0	0	0	0	0	0	0	0	0	0
p11	0,0003	2E-05	0,0002	2E-05	3E-10	0,0009	9E-08	0	0	0	2E-07	0,001
p12	4E-05	3E-06	2E-06	1E-07	6E-13	2E-05	3E-10	0	0	0	8E-10	0,0001
p13	2E-05	2E-06	1E-06	9E-08	4E-13	2E-05	2E-10	0	0	0	5E-10	8E-05
p14	4E-05	2E-06	2E-06	1E-07	5E-13	2E-05	2E-10	0	0	0	6E-10	0,0002
p15	3E-12	6E-14	2E-14	8E-16	3E-09	6E-13	6E-07	0	0	0	4E-18	9E-12
p16	0	0	0	0	0	0	0	0	0	0	0	0
p17	0	0	0	0	0	0	0	0	0	0	0	0
p18	0	0	0	0	0	0	0	0	0	0	0	0
p19	0	0	0	0	0	0	0	0	0	0	0	0
p20	0	0	0	0	0	0	0	0	0	0	0	0
p21	0	0	0	0	0	0	0	0	0	0	0	0
p22	0	0	0	0	0	0	0	0	0	0	0	0
p23	1E-07	1E-08	1E-05	2E-06	3E-11	5E-05	8E-09	0	0	0	2E-08	0,0003
p24	0	0	0	0	0	0	0	0	0	0	0	0
p25	3E-08	2E-09	2E-06	3E-07	4E-12	9E-06	1E-09	0	0	0	3E-09	0,0002
p26	1E-04	7E-06	5E-06	4E-07	2E-12	7E-05	9E-10	0	0	0	2E-09	0,0004
p27	2E-08	1E-06	3E-10	1E-11	7E-17	6E-09	2E-14	0	0	0	6E-05	7E-08
p28	7E-10	6E-08	1E-11	6E-13	0	3E-10	1E-15	0	0	0	3E-06	3E-09
p29	3E-06	0,0002	9E-08	6E-09	2E-14	2E-06	1E-11	0	0	0	3E-11	1E-05
p30	2E-08	2E-06	3E-10	1E-11	7E-17	6E-09	2E-14	0	0	0	6E-14	7E-08
p31	2E-06	0,0001	5E-08	3E-09	1E-14	1E-06	7E-12	0	0	0	2E-11	8E-06
p32	3E-10	2E-08	4E-12	2E-13	0	1E-10	4E-16	0	0	0	9E-16	1E-09
p33	1E-16	0	3E-16	3E-17	0	3E-16	1E-17	0	0	0	7E-19	3E-14
p34	0	0	0	0	0	0	0	0	0	0	0	0
p35	2E-05	1E-06	0,0021	0,0002	2E-09	0,0191	7E-07	0	0	0	2E-06	0,058
p36	7E-06	3E-07	0,0029	0,0004	4E-09	0,0073	1E-06	0	0	0	3E-06	3E-05
p37	3E-06	1E-07	0,0002	2E-05	2E-10	0,0021	7E-08	0	0	0	2E-07	1E-05
p38	0	0	0	0	0	0	0	0	0	0	0	0
p39	0	0	0	0	0	0	0	0	0	0	0	0
p40	3E-06	1E-07	0,0003	3E-05	2E-10	0,0023	8E-08	0	0	0	2E-07	0,0071

Simulation time length of 30 minutes

	x1	x2	x3	x4	x5	x6	x7	x8	x9	x10	x11	x12
x1	0,006342	0,008568	0,051927	0,026777	0,000854	0,021021	0,006615	0	0	0	0,012172	0,023914
x2	0,005097	0,008253	0,035322	0,017682	0,00034	0,016518	0,003115	0	0	0	0,005978	0,019237
x3	3,71E-05	0,00011	9,63E-05	3,32E-05	2,93E-05	0,000108	0,000113	0	0	0	0,000156	0,000332
x4	2,16E-05	5,9E-05	8,18E-05	3,5E-05	1,66E-05	6,4E-05	5,48E-05	0	0	0	6,81E-05	2,89E-05
x5	0,00034	0,000349	0,001795	0,00086	0,00405	0,00103	0,000111	0	0	0	0,000223	0,001247
x6	4,46E-05	0,000115	0,000157	6,41E-05	2,27E-05	0,000134	9,14E-05	0	0	0	0,000128	0,000399
x7	4,51E-05	3,72E-05	0,00018	8,14E-05	0,000962	0,000127	0,002775	0	0	0	1,52E-05	0,000138
x8	0	0	0	0	0	0	0	0	0	0	0	0
x9	0	0	0	0	0	0	0	0	0	0	0	0
x10	0	0	0	0	0	0	0	0	0	0	0	0
x11	0	0	0	0	0	0	0	0	0	0	0	0
x12	0	0	0	0	0	0	0	0	0	0	0	0
p1	0,0061	0,015	0,0392	0,0195	0,0003	0,0194	0,0032	0	0	0	0,0062	0,0231
p2	0,0053	0,0133	0,0359	0,0179	0,0003	0,017	0,0031	0	0	0	0,006	0,0199
p3	0,0029	0,0071	0,0816	0,0416	0,0011	0,0365	0,009	0	0	0	0,0168	0,0418
p4	0,0003	0,0012	0,0538	0,0005	0,0003	0,0009	0,0015	0	0	0	0,0024	0,0019
p5	0,0004	0,0018	0,0139	0,0132	0,0004	0,0011	0,0031	0	0	0	0,0057	0,0013
p6	0,0003	0,0014	0,0111	0,0136	0,0003	0,0008	0,0026	0	0	0	0,005	0,0012
p7	0,0009	0,0037	0,0027	0,0011	0,0008	0,0023	0,0062	0	0	0	0,0114	0,0033
p8	0,0004	0,0019	0,0423	0,0212	0,0004	0,001	0,0037	0	0	0	0,0072	0,0023
p9	0,0009	0,0045	0,0967	0,0482	0,0009	0,0024	0,0085	0	0	0	0,0164	0,0035
p10	0	0	0	0	0	0	0	0	0	0	0	0
p11	0,0046	0,0046	0,0235	0,0112	0,0001	0,0137	0,0014	0	0	0	0,0028	0,0171
p12	0,0006	0,0006	0,003	0,0014	2E-05	0,0017	0,0002	0	0	0	0,0004	0,0021
p13	0,0004	0,0004	0,002	0,001	1E-05	0,0012	0,0001	0	0	0	0,0002	0,0015
p14	0,0019	0,0019	0,0095	0,0045	5E-05	0,0056	0,0005	0	0	0	0,0011	0,007
p15	4E-05	2E-05	0,0001	4E-05	0,0014	1E-04	0,0053	0	0	0	5E-06	0,0001
p16	0	0	0	0	0	0	0	0	0	0	0	0
p17	0	0	0	0	0	0	0	0	0	0	0	0
p18	0	0	0	0	0	0	0	0	0	0	0	0
p19	0	0	0	0	0	0	0	0	0	0	0	0
p20	0	0	0	0	0	0	0	0	0	0	0	0
p21	0	0	0	0	0	0	0	0	0	0	0	0
p22	0	0	0	0	0	0	0	0	0	0	0	0
p23	4E-07	1E-06	4E-06	2E-06	2E-07	3E-06	7E-07	0	0	0	1E-06	0,0001
p24	0	0	0	0	0	0	0	0	0	0	0	0
p25	7E-08	2E-07	7E-07	3E-07	4E-08	4E-07	1E-07	0	0	0	2E-07	5E-05
p26	0,0017	0,0017	0,0087	0,0041	5E-05	0,0051	0,0005	0	0	0	0,001	0,0063
p27	0,0007	0,0028	0,0023	0,001	3E-06	0,0019	6E-05	0	0	0	0,0078	0,0027
p28	5E-06	2E-05	2E-05	9E-06	4E-08	1E-05	7E-07	0	0	0	5E-05	1E-05
p29	0,0009	0,0027	0,0042	0,002	1E-05	0,0027	0,0002	0	0	0	0,0004	0,0039
p30	0,0009	0,004	0,0028	0,0012	4E-06	0,0024	8E-05	0	0	0	0,0002	0,0034
p31	0,0011	0,0042	0,0044	0,002	1E-05	0,0032	0,0002	0	0	0	0,0004	0,0033
p32	4E-05	0,0002	1E-04	4E-05	1E-07	9E-05	2E-06	0	0	0	5E-06	0,0001
p33	7E-15	3E-15	1E-12	4E-15	1E-15	6E-09	1E-16	0	0	0	5E-16	2E-05
p34	0	0	0	0	0	0	0	0	0	0	0	0
p35	0,0027	0,0066	0,0776	0,0396	0,001	0,0326	0,0086	0	0	0	0,016	0,0372
p36	0,0015	0,0011	0,0073	0,0036	0,0002	0,0402	0,0011	0	0	0	0,0019	0,0056
p37	0,0003	0,0008	0,0097	0,0049	0,0001	0,0045	0,001	0	0	0	0,0019	0,0012
p38	0	0	0	0	0	0	0	0	0	0	0	0
p39	0	0	0	0	0	0	0	0	0	0	0	0
p40	0,0004	0,0008	0,0107	0,0054	0,0001	0,0049	0,0011	0	0	0	0,0021	0,0057

Simulation time length of 60 minutes

	x1	x2	x3	x4	x5	x6	x7	x8	x9	x10	x11	x12
x1	0,001583	0,000482	0,013996	0,007747	0,003486	0,005759	0,010249	0	0	0	0,012492	0,00597
x2	0,001914	0,001699	0,014058	0,007597	0,001878	0,006615	0,006452	0	0	0	0,008694	0,007077
x3	4,4E-05	7,34E-05	0,000232	0,000118	4,93E-05	0,000141	5,73E-05	0	0	0	7,47E-07	0,00016
x4	2,25E-05	3,61E-05	0,000122	6,25E-05	2,51E-05	7,25E-05	2,46E-05	0	0	0	7,42E-06	0,00011
x5	0,000385	0,000382	0,001956	0,000996	0,003114	0,001214	0,000397	0	0	0	0,000615	0,001476
x6	4,35E-05	6,97E-05	0,000237	0,000122	3,71E-05	0,00014	3,51E-05	0	0	0	1,71E-05	0,000158
x7	0,000114	0,000108	0,000488	0,00024	0,001509	0,000345	0,002138	0	0	0	9,92E-05	0,000424
x8	0	0	0	0	0	0	0	0	0	0	0	0
x9	0	0	0	0	0	0	0	0	0	0	0	0
x10	0	0	0	0	0	0	0	0	0	0	0	0
x11	0	0	0	0	0	0	0	0	0	0	0	0
x12	0	0	0	0	0	0	0	0	0	0	0	0
p1	0,004	0,0119	0,023	0,012	0,002	0,0131	0,0075	0	0	0	0,0106	0,0153
p2	0,0029	0,0095	0,0178	0,0094	0,0019	0,0095	0,0068	0	0	0	0,0093	0,0105
p3	0,0066	0,0132	0,0271	0,0148	0,005	0,0126	0,0156	0	0	0	0,0198	0,0136
p4	0,0005	0,0008	0,0384	0,003	0,0005	0,0016	0,0005	0	0	0	0,0004	0,0019
p5	0,0014	0,0034	0,0129	0,0063	0,0017	0,0043	0,0054	0	0	0	0,0069	0,0053
p6	0,0013	0,0032	0,0023	0,0065	0,0015	0,0038	0,0052	0	0	0	0,007	0,0048
p7	0,0029	0,0068	0,0123	0,006	0,0034	0,0087	0,0105	0	0	0	0,0133	0,0108
p8	0,0018	0,0045	0,0159	0,0087	0,0022	0,0055	0,0077	0	0	0	0,0103	0,0069
p9	0,0044	0,0112	0,0549	0,0288	0,0053	0,0131	0,0189	0	0	0	0,0262	0,0165
p10	0	0	0	0	0	0	0	0	0	0	0	0
p11	0,0061	0,006	0,0301	0,0152	0,0012	0,0191	0,0055	0	0	0	0,0086	0,0231
p12	0,0006	0,0006	0,0032	0,0016	0,0001	0,002	0,0007	0	0	0	0,001	0,0023
p13	0,0007	0,0007	0,0031	0,0016	0,0001	0,0021	0,0005	0	0	0	0,0008	0,0026
p14	0,0021	0,0022	0,0108	0,0055	0,0005	0,0067	0,0021	0	0	0	0,0033	0,0084
p15	0,0003	0,0003	0,0011	0,0005	0,0058	0,0009	0,0084	0	0	0	0,0001	0,0013
p16	0	0	0	0	0	0	0	0	0	0	0	0
p17	0	0	0	0	0	0	0	0	0	0	0	0
p18	0	0	0	0	0	0	0	0	0	0	0	0
p19	0	0	0	0	0	0	0	0	0	0	0	0
p20	0	0	0	0	0	0	0	0	0	0	0	0
p21	0	0	0	0	0	0	0	0	0	0	0	0
p22	0	0	0	0	0	0	0	0	0	0	0	0
p23	3E-07	4E-07	4E-06	2E-06	3E-07	2E-06	1E-07	0	0	0	8E-07	9E-06
p24	0	0	0	0	0	0	0	0	0	0	0	0
p25	5E-08	6E-08	7E-07	4E-07	4E-08	4E-07	2E-08	0	0	0	1E-07	7E-06
p26	0,0023	0,0022	0,011	0,0055	0,0004	0,0071	0,002	0	0	0	0,0032	0,0086
p27	0,0016	0,0032	0,0073	0,0037	0,0001	0,0049	0,0009	0	0	0	0,003	0,0062
p28	1E-05	3E-05	5E-05	3E-05	1E-06	4E-05	7E-06	0	0	0	6E-05	0,0004
p29	0,0012	0,0025	0,006	0,0031	0,0002	0,0038	0,001	0	0	0	0,0017	0,0045
p30	0,0029	0,0072	0,0126	0,0062	0,0002	0,0089	0,0013	0	0	0	0,0023	0,011
p31	0,0027	0,0066	0,0122	0,006	0,0002	0,0084	0,0014	0	0	0	0,0025	0,0101
p32	0,0002	0,0005	0,0008	0,0004	8E-06	0,0006	6E-05	0	0	0	0,0001	0,0007
p33	2E-15	8E-15	3E-13	1E-14	3E-16	1E-09	2E-16	0	0	0	5E-15	5E-06
p34	0	0	0	0	0	0	0	0	0	0	0	0
p35	0,006	0,0118	0,0211	0,0117	0,0047	0,0084	0,0144	0	0	0	0,0182	0,0085
p36	0,0018	0,0018	0,008	0,004	0,0006	0,0266	0,0021	0	0	0	0,0028	0,0068
p37	0,0008	0,0016	0,0053	0,0028	0,0006	0,003	0,002	0	0	0	0,0026	0,003
p38	0	0	0	0	0	0	0	0	0	0	0	0
p39	0	0	0	0	0	0	0	0	0	0	0	0
p40	0,0009	0,0017	0,0058	0,003	0,0006	0,0033	0,0021	0	0	0	0,0029	0,0038

Simulation time length of 100 minutes

	x1	x2	x3	x4	x5	x6	x7	x8	x9	x10	x11	x12
x1	0,000922	0,001822	0,002426	0,001131	0,006247	0,002728	0,008104	0	0	0	0,003919	0,003564
x2	0,000265	0,000775	0,00017	8,3E-06	0,00386	0,000662	0,00569	0	0	0	0,003506	0,001
x3	2,24E-05	2,91E-05	8,86E-05	4,62E-05	4,75E-05	7,32E-05	1,17E-05	0	0	0	4,29E-05	0,000156
x4	1,07E-05	1,34E-05	4,27E-05	2,23E-05	2,27E-05	3,5E-05	2,72E-06	0	0	0	2,36E-05	2,98E-05
x5	0,000306	0,000324	0,001105	0,000565	0,002067	0,000974	0,000581	0	0	0	0,000595	0,001144
x6	1,93E-05	2,43E-05	7,85E-05	4,11E-05	3,13E-05	6,36E-05	3,42E-06	0	0	0	4,57E-05	0,00016
x7	0,000183	0,000196	0,000598	0,000299	0,001796	0,000566	0,001451	0	0	0	0,000196	0,000686
x8	0	0	0	0	0	0	0	0	0	0	0	0
x9	0	0	0	0	0	0	0	0	0	0	0	0
x10	0	0	0	0	0	0	0	0	0	0	0	0
x11	0	0	0	0	0	0	0	0	0	0	0	0
x12	0	0	0	0	0	0	0	0	0	0	0	0
p1	0,0022	0,0081	0,0082	0,0043	0,0047	0,007	0,0082	0	0	0	0,0067	0,0082
p2	0,0014	0,0063	0,0055	0,0029	0,0042	0,0046	0,0069	0	0	0	0,0052	0,0054
p3	0,0072	0,0118	0,0001	0,0002	0,0095	0,0006	0,0132	0	0	0	0,0075	0,001
p4	0,0002	0,0001	0,018	0,0009	0,0004	0,0006	0,0003	0	0	0	0,0011	0,0006
p5	0,0017	0,0031	0,0086	0,002	0,0034	0,0054	0,0053	0	0	0	0,0037	0,0065
p6	0,0016	0,003	0,0027	0,0012	0,0032	0,0051	0,005	0	0	0	0,0034	0,0061
p7	0,0034	0,0061	0,0117	0,0059	0,0066	0,0106	0,0098	0	0	0	0,0065	0,0126
p8	0,0023	0,004	0,0006	0,0002	0,0046	0,0071	0,0066	0	0	0	0,0039	0,0085
p9	0,0062	0,0117	0,017	0,0089	0,0118	0,0193	0,02	0	0	0	0,0157	0,0232
p10	0	0	0	0	0	0	0	0	0	0	0	0
p11	0,0066	0,0069	0,0228	0,0115	0,0039	0,0205	0,0091	0	0	0	0,01	0,0247
p12	0,0004	0,0005	0,0016	0,0008	0,0004	0,0014	0,0009	0	0	0	0,0009	0,0017
p13	0,0011	0,0011	0,0035	0,0018	0,0004	0,0034	0,001	0	0	0	0,0012	0,0042
p14	0,0015	0,0017	0,0057	0,0029	0,0014	0,0049	0,0031	0	0	0	0,0032	0,0058
p15	0,0009	0,0009	0,0027	0,0013	0,0105	0,0027	0,0063	0	0	0	0,0007	0,0033
p16	0	0	0	0	0	0	0	0	0	0	0	0
p17	0	0	0	0	0	0	0	0	0	0	0	0
p18	0	0	0	0	0	0	0	0	0	0	0	0
p19	0	0	0	0	0	0	0	0	0	0	0	0
p20	0	0	0	0	0	0	0	0	0	0	0	0
p21	0	0	0	0	0	0	0	0	0	0	0	0
p22	0	0	0	0	0	0	0	0	0	0	0	0
p23	3E-08	1E-07	8E-07	4E-07	3E-08	6E-07	5E-07	0	0	0	8E-07	1E-05
p24	0	0	0	0	0	0	0	0	0	0	0	0
p25	5E-09	2E-08	1E-07	8E-08	5E-09	1E-07	9E-08	0	0	0	1E-07	9E-06
p26	0,0024	0,0026	0,0083	0,0042	0,0014	0,0077	0,0033	0	0	0	0,0037	0,0092
p27	0,0007	0,0008	0,003	0,0016	0,0007	0,0024	0,0017	0	0	0	0,0036	0,0026
p28	1E-05	3E-05	5E-05	2E-05	5E-06	4E-05	1E-05	0	0	0	6E-05	7E-05
p29	0,0009	0,0018	0,0033	0,0017	0,0007	0,0029	0,0016	0	0	0	0,0018	0,0035
p30	0,003	0,0058	0,0106	0,0054	0,0011	0,0094	0,0033	0	0	0	0,0043	0,0112
p31	0,0028	0,0058	0,0101	0,0051	0,0012	0,009	0,0033	0	0	0	0,0041	0,0107
p32	0,0002	0,0005	0,0008	0,0004	6E-05	0,0007	0,0002	0	0	0	0,0003	0,0009
p33	5E-16	8E-16	1E-14	3E-15	1E-15	1E-10	1E-15	0	0	0	8E-15	4E-07
p34	0	0	0	0	0	0	0	0	0	0	0	0
p35	0,006	0,0098	0,0037	0,0018	0,0086	0,004	0,0114	0	0	0	0,0056	0,0051
p36	0,0015	0,0016	0,0049	0,0025	0,0015	0,0163	0,0028	0	0	0	0,0026	0,0055
p37	0,001	0,0017	0,0025	0,0013	0,0013	0,0022	0,0021	0	0	0	0,0017	0,0039
p38	0	0	0	0	0	0	0	0	0	0	0	0
p39	0	0	0	0	0	0	0	0	0	0	0	0
p40	0,0011	0,0019	0,0027	0,0014	0,0014	0,0024	0,0023	0	0	0	0,0019	0,003

Simulation time length of 1440 minutes

	x1	x2	x3	x4	x5	x6	x7	x8	x9	x10	x11	x12
x1	3,56E-07	5,05E-07	8,54E-07	4,35E-07	1,05E-06	8,46E-07	6,55E-07	0	0	0	4,89E-07	0,000247
x2	2,62E-07	3,71E-07	6,36E-07	3,23E-07	8,14E-07	6,77E-07	4,32E-07	0	0	0	3,57E-07	1,47E-06
x3	8,18E-11	3,66E-11	5,51E-10	2,64E-10	2,85E-09	9,86E-11	2,98E-09	0	0	0	1,01E-10	2,34E-06
x4	1,53E-10	1,76E-10	5,47E-10	2,7E-10	1,77E-09	1,43E-09	1,31E-09	0	0	0	1,01E-10	8,23E-06
x5	2,75E-08	3,5E-08	8,35E-08	4,17E-08	2,1E-07	9,76E-08	1,04E-07	0	0	0	2,71E-08	1,59E-05
x6	7,29E-10	9,61E-10	2,07E-09	1,04E-09	4,52E-09	1,61E-08	1,51E-09	0	0	0	8,06E-10	5,5E-05
x7	7,41E-08	1,05E-07	1,76E-07	8,99E-08	2,07E-07	1,89E-07	1,5E-07	0	0	0	1,03E-07	7,5E-06
x8	0	0	0	0	0	0	0	0	0	0	0	0
x9	0	0	0	0	0	0	0	0	0	0	0	0
x10	0	0	0	0	0	0	0	0	0	0	0	0
x11	0	0	0	0	0	0	0	0	0	0	0	0
x12	0	0	0	0	0	0	0	0	0	0	0	0
p1	0,0015	0,0061	0,0041	0,0021	0,0043	0,0046	0,0029	0	0	0	0,0017	0,0056
p2	0,0012	0,0048	0,0033	0,0017	0,0035	0,0037	0,0024	0	0	0	0,0014	0,0044
p3	0,0036	0,0058	0,0049	0,0024	0,0051	0,0054	0,0035	0	0	0	0,002	0,0066
p4	4E-08	5E-08	0,0107	6E-08	1E-07	9E-08	6E-08	0	0	0	6E-08	7E-06
p5	0,0011	0,002	0,0047	0,0016	0,0034	0,0036	0,0023	0	0	0	0,0013	0,0043
p6	0,0008	0,0014	0,0008	0,0012	0,0025	0,0026	0,0017	0	0	0	0,001	0,0031
p7	0,0019	0,0033	0,0055	0,0028	0,0058	0,0061	0,0039	0	0	0	0,0023	0,0072
p8	0,0006	0,001	0,0017	0,0009	0,0018	0,0019	0,0012	0	0	0	0,0007	0,0022
p9	0,0043	0,0075	0,0121	0,0061	0,0127	0,0135	0,0087	0	0	0	0,005	0,0161
p10	0	0	0	0	0	0	0	0	0	0	0	0
p11	0,0065	0,0085	0,0186	0,0093	0,0194	0,0204	0,0133	0	0	0	0,0076	0,0244
p12	0,0003	0,0004	0,0008	0,0004	0,0008	0,0009	0,0006	0	0	0	0,0003	0,001
p13	0,0013	0,0017	0,0036	0,0018	0,0037	0,004	0,0025	0	0	0	0,0015	0,0048
p14	0,0009	0,0012	0,0026	0,0013	0,0027	0,0028	0,0018	0	0	0	0,001	0,0034
p15	3E-06	3E-06	7E-06	4E-06	2E-05	8E-06	4E-06	0	0	0	3E-06	9E-05
p16	0	0	0	0	0	0	0	0	0	0	0	0
p17	0	0	0	0	0	0	0	0	0	0	0	0
p18	0	0	0	0	0	0	0	0	0	0	0	0
p19	0	0	0	0	0	0	0	0	0	0	0	0
p20	0	0	0	0	0	0	0	0	0	0	0	0
p21	0	0	0	0	0	0	0	0	0	0	0	0
p22	0	0	0	0	0	0	0	0	0	0	0	0
p23	2E-11	3E-11	7E-11	4E-11	5E-11	2E-09	8E-11	0	0	0	4E-11	8E-06
p24	0	0	0	0	0	0	0	0	0	0	0	0
p25	4E-12	6E-12	1E-11	7E-12	9E-12	2E-09	1E-11	0	0	0	8E-12	6E-06
p26	0,0025	0,0032	0,0069	0,0035	0,0072	0,0077	0,0049	0	0	0	0,0028	0,0092
p27	8E-08	1E-07	3E-07	1E-07	6E-07	3E-07	3E-07	0	0	0	3E-09	2E-06
p28	1E-05	3E-05	3E-05	2E-05	4E-05	4E-05	2E-05	0	0	0	7E-05	5E-06
p29	0,0007	0,0016	0,0019	0,0009	0,0019	0,0021	0,0013	0	0	0	0,0008	0,0027
p30	0,0007	0,0017	0,002	0,001	0,0021	0,0022	0,0014	0	0	0	0,0008	0,0026
p31	0,0011	0,0028	0,0032	0,0016	0,0034	0,0036	0,0023	0	0	0	0,0013	0,0042
p32	3E-05	7E-05	8E-05	4E-05	9E-05	9E-05	6E-05	0	0	0	3E-05	1E-04
p33	8E-09	2E-08	1E-07	6E-08	8E-08	1E-07	2E-07	0	0	0	7E-08	2E-06
p34	0	0	0	0	0	0	0	0	0	0	0	0
p35	0,0023	0,0037	0,0032	0,0016	0,0033	0,0035	0,0023	0	0	0	0,0013	0,0042
p36	0,0009	0,0011	0,0025	0,0012	0,0026	0,013	0,0018	0	0	0	0,001	0,0032
p37	0,0012	0,0019	0,0016	0,0008	0,0017	0,0018	0,0011	0	0	0	0,0007	0,0046
p38	0	0	0	0	0	0	0	0	0	0	0	0
p39	0	0	0	0	0	0	0	0	0	0	0	0
p40	0,0013	0,0021	0,0017	0,0009	0,0018	0,0019	0,0013	0	0	0	0,0007	0,0024

F. Figures sensitivity analysis of a normal patient

Delta state figures of the first ten parameters and the first four states of a normal patient with a simulation duration of 100 minutes.

x₀(1)

x₀(2)